Development/Plasticity/Repair

Hoxb8 Intersection Defines a Role for *Lmx1b* in Excitatory Dorsal Horn Neuron Development, Spinofugal Connectivity, and Nociception

Nora E. Szabo,[1] Ronan V. da Silva,[1,2] Susana G. Sotocinal,[3] Hanns Ulrich Zeilhofer,[4] Jeffrey S. Mogil,[3] and Artur Kania[1,2,5]

[1]Institut de Recherches Cliniques de Montréal, Montréal, Quebec H2W 1R7, Canada, [2]Integrated Program in Neuroscience, McGill University, Montréal, Quebec H3A 2B2, Canada, [3]Department of Psychology and Alan Edwards Center for Research on Pain, McGill University, Montreal, Quebec H3A 1B1, Canada, [4]Institute of Pharmacology and Toxicology, University of Zurich, and Institute of Pharmaceutical Sciences, Swiss Federal Institute of Technology Zurich, 8092 Zurich, Switzerland, and [5]Departments of Anatomy and Cell Biology, and Biology, Division of Experimental Medicine, McGill University Montréal, Quebec, H3A 2B2 and Faculté de Médecine, Université de Montréal, Montréal, Quebec H3C 3J7, Canada

Spinal cord neurons respond to peripheral noxious stimuli and relay this information to higher brain centers, but the molecules controlling the assembly of such pathways are poorly known. In this study, we use the intersection of *Lmx1b* and *Hoxb8::Cre* expression in the spinal cord to genetically define nociceptive circuits. Specifically, we show that Lmx1b, previously shown to be expressed in glutamatergic dorsal horn neurons and critical for dorsal horn development, is expressed in nociceptive dorsal horn neurons and that its deletion results in the specific loss of excitatory dorsal horn neurons by apoptosis, without any effect on inhibitory neuron numbers. To assess the behavioral consequences of *Lmx1b* deletion in the spinal cord, we used the brain-sparing driver *Hoxb8::Cre*. We show that such a deletion of *Lmxb1* leads to a robust reduction in sensitivity to mechanical and thermal noxious stimulation. Furthermore, such conditional mutant mice show a loss of a subpopulation of glutamatergic dorsal horn neurons, abnormal sensory afferent innervations, and reduced spinofugal innervation of the parabrachial nucleus and the periaqueductal gray, important nociceptive structures. Together, our results demonstrate an important role for the intersection of *Lmx1b* and *Hoxb8::cre* expression in the development of nociceptive dorsal horn circuits critical for mechanical and thermal pain processing.

Key words: **dorsal horn; Hoxb8:: Cre; Lmx1b; mouse; nociception; projection neurons**

Introduction

How neural circuits transform noxious stimuli into pain perception has been studied extensively, but the molecules controlling the assembly of such circuits have remained elusive. Noxious stimuli, such as cold, heat, and pinch, activate subsets of dorsal root ganglion (DRG) neurons (Caterina et al., 1997; Bautista et al., 2007; Basbaum et al., 2009), which project to discrete dorsal horn laminae, correlating with modality-specific responses of dorsal horn neurons (Cavanaugh et al., 2009; Todd, 2010). This argues for nociceptive "labeled lines" dedicated to particular pain modalities (Craig, 2003), but the molecular determinants of central modality-specific circuit organization are scarce (Braz et al., 2005). In the spinal cord, nociceptive signals are relayed by either modality-specific or multimodal wide dynamic range projection neurons (Dado et al., 1994) to higher brain centers, such as the parabrachial nucleus (Pb), the periaqueductal gray (PAG), and several thalamic nuclei (Al-Khater and Todd, 2009; Todd, 2010). These regions act in concert to process the complex aspects of pain, such as its sensory and affective dimensions (Basbaum and Bushnell, 2008), but their relative contributions to nocifensive behaviors remain obscure.

Developmental studies have shown that spinal-level nociceptive responses can be elicited as early as E18.5, suggesting that dorsal horn nociceptive connectivity occurs early in development (Narayanan et al., 1971), similar to spinothalamic connectivity (Davidson et al., 2010a). The molecular cascades coordinating dorsal horn neuron development are starting to be uncovered (Helms and Johnson, 2003) and one instance with clear links between them and neuronal function is the specification of neurotransmitter phenotype of neurons, which is determined by combinations of transcription factors imposing either a glutama-

Received Nov. 13, 2014; revised Feb. 17, 2015; accepted Feb. 21, 2015.

Author contributions: N.E.S. and A.K. designed research; N.E.S., R.V.S., and S.G.S. performed research; S.G.S., H.U.Z., and J.S.M. contributed unpublished reagents/analytic tools; N.E.S., R.V.S., J.S.M., and A.K. analyzed data; N.E.S., R.V.S., H.U.Z., J.S.M., and A.K. wrote the paper.

This work was supported by Reseau Québecois de recherche sur la douleur, Canadian Institutes of Health Research, Canada Foundation for Innovation, Brain Canada, and the W. Garfield Weston Foundation to A.K. and a McGill/Center for Neuroscience Zurich collaborative project grant to A.K. and H.U.Z., N.E.S. was supported by a Deutscher Akademischer Austausch Dienst scholarship and a Institut de Recherches Cliniques de Montréal Pizzagalli fellowship. We thank Randy L. Johnson for providing the Lmx1b conditional allele; Tom Jessell and Jean Vacher for providing antibodies; Farin Bourojeni and other members of the A.K. laboratory; Yves De Koninck, Hendrik Wildner, and Tomomi Shimogori for comments on the manuscript and discussions; and Meirong Liang, Julie Cardin, Dominic Filion, and Isabelle Brisson for technical assistance.

The authors declare no competing financial interests.

Correspondence should be addressed to Dr. Artur Kania, Institut de Recherches Cliniques de Montréal, 110, avenue des Pins Ouest, Montréal, QC H2W 1R7, Canada. E-mail: artur.kania@ircm.qc.ca.

DOI:10.1523/JNEUROSCI.4690-14.2015

 0270-6474/15/355233-14$15.00/0

tergic excitatory or a GABAergic/glycinergic inhibitory identity (Cheng et al., 2004, 2005; Mizuguchi et al., 2006). Lmx1b is a LIM-homeobox transcription factor, essential for dorsal horn development that has been proposed to function downstream of glutamatergic-fate determinants by sustaining the expression of transcription factors, such as Drg11 (Ding et al., 2004). Lmx1b is also required for the survival of midbrain serotonergic and trigeminal neurons, as well as for trigeminothalamic connectivity (Zhao et al., 2006; Xiang et al., 2010). In humans, *LMX1B* mutations cause the Nail-Patella Syndrome (NPS) characterized by limb and kidney malformations (Dreyer et al., 1998) with apparent deficits in mechanical nociception (Dunston et al., 2005), suggesting that Lmx1b is important for the development of nociceptive circuits.

Here, we use the brain-sparing *HoxB8::Cre* transgene (Witschi et al., 2010) to conditionally ablate *Lmx1b* in spinal neurons. We show that this spinal cord-specific ablation of *Lmx1b* results in reduced sensitivity to noxious mechanical and thermal stimulation, disrupted spinofugal connectivity, and abnormal sensory afferent innervation. Our study thus establishes the intersection of *Lmx1b* and *Hoxb8* as a genetic definition of nociception.

Materials and Methods

Mouse lines. Mice were housed (Borodinsky et al., 2004) in the animal care facilities of Institut de Recherches Cliniques de Montréal. Animals were kept on a 12 h light/dark cycle, with food and water provided *ad libitum*. All experimental procedures were approved by the Animal Care and Use Committees at McGill University and Institut de Recherches Cliniques de Montréal, in accordance with the regulations of the Canadian Council on Animal Care.

Lmx1b knock-out mouse and Lmx1b conditional mouse. The *Lmx1b*-null and the $Lmx1b^{fl}$ alleles were described previously (Chen et al., 1998; Zhao et al., 2006). *Hoxb8::Cre* mice (Witschi et al., 2010) were crossed to the $Lmx1b^{fl}$ allele to produce *Hoxb8::Cre*$^{+/-}$; $Lmx1b^{fl/fl}$ conditional *Lmx1b*-deficient mice ($Lmx1b^{CND}$). Only mice heterozygous for *Hoxb8::Cre* and homozygous for the $Lmx1b^{fl}$ allele were analyzed as $Lmx1b^{CND}$ mutants. Control mice were either $Lmx1b^{fl/+}$ or $Lmx1b^{fl/fl}$ mice ($Lmx1b^{CTL}$). $Lmx1b^{CND}$ were also analyzed in the context of the *Rosa26:lox:tdTomato:lox:GFP*, which we abbreviate *R26mGFP*, or the *Rosa26:lox:Stop:lox:YFP* transgene (The Jackson Laboratory), which we abbreviate *R26YFP*, allowing the expression of a membrane-targeted GFP or YFP in a Cre-dependent manner.

Mouse behavior. Adult $Lmx1b^{CND}$ mice and their $Lmx1b^{CTL}$ littermates, of either sex, were used for all behavioral experiments. The mice were accommodated to the testing room for at least 60 min before testing commenced.

In the thermal nociception paw withdrawal (Hargreaves') test, a radiant heat source was focused on the plantar surface of left and right forepaw, and the latency to withdraw the paw from the heat source was recorded in seconds (Hargreaves et al., 1988). We used the forepaw instead of the more common hindpaw because $Lmx1b^{CND}$ mice show abnormal and shortened hindlimbs, whereas the forelimbs were normal. For the tail-immersion test, mice were gently restrained in a cloth/cardboard container, the tip of the tail (one-third of the length) immersed in hot water (49°C and 51°C), and the latency of tail withdrawal was monitored in seconds (Ben-Bassat et al., 1959; Mogil et al., 2006).

In the von Frey mechanical nociception assay, mice were stimulated with nylon monofilaments, and withdrawal thresholds were measured using the up-and-down method of Dixon (Chaplan et al., 1994). Calibrated monofilaments (0.008–4.0 g) were applied to the plantar side of the animal's forepaws and tail base. If upon stimulation with the 0.4 g filament a paw withdrawal response was not elicited, a stronger stimulation was applied or, if the withdrawal response was detected, a weaker stimulus was used. The responses were tabulated and the 50% response threshold determined.

For the paw pinch assay, a clip with a force of 80 g at the tip was put on one forepaw and the latency in seconds until the mouse showed an aversive response, such as licking, biting, or shaking of the forepaw, was recorded. The cutoff time was 2 min. After a rest of at least 15 min, the other forepaw was tested.

For the weights test, steel wires were used with an increasing number of steel chain links attached to them, resulting in the following weights: 20 g (weight score of 3), 33 g (score of 6), 46 g (score of 9), 59 g (score of 12), 72 g (score of 15), 85 g (score of 18), and 98 g (score of 21). The mouse was held by the tail and lifted up after it grabbed the steel wire with its forepaws. If the mouse could hold the weight with its forepaws for 3 s, the next heavier weight was tested until the heaviest weight it could hold on to was reached (Deacon, 2013).

For statistical analysis of behavioral data, the Student's unpaired *t*-test was performed. p values <0.05 were considered statistically significant.

c-Fos induction. To investigate *c-Fos* expression induced by thermal stimulation, mice were anesthetized with a mixture of ketamine/xylazine and the forepaw immersed in a 52°C water bath for 10 s. This was repeated every minute for 10 min. Mice recovered full consciousness after the paw immersion and, 2 h after the experiment, were reanesthetized and perfused.

For mechanical stimulation, an alligator clamp was used to pinch glabrous skin of the forepaw 3 times for 30 s with 30 s intervals. The applied force by the alligator clamp was ~300 g. The mechanical stimuli were applied without anesthesia. Two hours after stimulation, mice were anesthetized with ketamine/xylazine and perfused with 4% PFA. The spinal cords were dissected and postfixed in 4% PFA for 2 h, equilibrated with 30% sucrose in PBS overnight, embedded in O.C.T. (Sakura Finetek), and stored at −80°C.

Fluorogold (FG) injection. Thalamic injections of FG (Fluorochrome) for retrograde labeling of spinothalamic tract neurons were performed in neonatal mouse pups *in vivo* (Davidson et al., 2010b). Pups were placed on crushed ice for 2 min for hypothermia-induced anesthesia. A fine glass pipette was inserted through the skull to the location of the thalamus, and ~200 nl of 4% FG was injected using a microinjector (Narishige, IM-300 Microinjector). The pups were placed on a warming pad to recover immediately after the procedure, and anesthetized and perfused 3–4 d after the injection. The spinal cords and brains were dissected and postfixed in 4% PFA for 2 h, equilibrated with 30% sucrose in PBS overnight, embedded in O.C.T. (Sakura Finetek), and stored at −80°C. FG-positive spinal cord neurons were visualized by performing immunohistochemistry with rabbit anti-FG antibody (1:500, Fluorochrome), and the brains of the injected pups were analyzed to confirm correct targeting of the tracer injection.

In situ *hybridization.* cRNA probes were generated as follows: target sequence amplification primers were designed using Primer3 version 0.4.0 software (Rozen and Skaletsky, 2000) with a probe size set at 600–800 bp. One-step RT-PCR was performed (QIAGEN) using appropriate primers containing T7 polymerase promoters (Invitrogen) to make and amplify cDNA template from mouse E11.5 pooled brain RNA. The PCR product was purified by gel electrophoresis in 1% agarose gel and gel extraction using QIAquick gel extraction kit (QIAGEN). The purified DNA was then reamplified by PCR. The yield of DNA was estimated using the low DNA mass ladder (Invitrogen) after gel electrophoresis. DIG-labeled RNA probes were synthesized by *in vitro* transcription with T7 RNA polymerase using DIG RNA labeling kit (Roche). All probes were verified by sequencing.

In situ mRNA detection was performed as described previously (Schaeren-Wiemers and Gerfin-Moser, 1993; Kao and Kania, 2011). In brief, tissue sections were first fixed in 4% PFA in PBS for 10 min at room temperature, washed three times with PBS for 5 min, and digested in proteinase K solution: 1 μg/ml proteinase K (Roche) in 6.25 mM EDTA, pH 8.0 (Invitrogen), and 50 mM Tris, pH 7.5 (Fisher Scientific). Samples were acetylated for 10 min by immersion in a mixture of 6 ml of triethanolamine (Sigma), 500 ml of double-distilled H_2O, and 1.30 ml of acetic anhydride (Sigma). After PBS washes, samples were incubated with hybridization buffer [50% formamide, 5× SSC (20× SSC is 3 M NaCl, 0.3 M NaAc), 5× Denhardt's (Sigma), and 500 μg/ml Salmon sperm DNA (Roche)] for 2 h at room temperature followed by incubation overnight at 72°C with DIG-labeled RNA probes (see above) in the hybridization buffer at a concentration of 2–5 ng/μl. After hybridization, samples were

immersed in 5× SSC at 72°C, followed by two washes in 0.2× SSC at 72°C for 45 min each and 0.2× SSC at room temperature for 5 min. Tissues were then rinsed with B1 buffer [0.1 M Tris, pH 7.5, and 0.15 M NaCl (Fisher Scientific)] for 5 min, blocked with B2 buffer (10% heat inactivated horse serum in B1) for 1 h at room temperature, and incubated with anti-DIG antibody (1:5000 in B2, Roche) overnight at 4°C. Samples were then rinsed with B1 and equilibrated with B3 buffer: 0.1 M Tris, pH 9.5, 0.1 M NaCl, 0.05 M $MgCl_2$ (Fisher Scientific). To detect bound anti-DIG antibodies, samples were incubated with B4 buffer [100 mg/ml NBT, 50 mg/ml BCIP (Roche) and 400 mM levamisol (Sigma) in B3] in the dark. The reaction was stopped by immersion in H_2O.

Immunohistochemistry. Mouse embryos were fixed in 4% PFA (Sigma) in PBS, equilibrated with 30% sucrose in PBS overnight, embedded in O.C.T. (Sakura Finetek), and stored at −80°C. Twenty micrometer sections were collected using a Leica cryostat microtome. Sectioned tissue was first washed in PBS, incubated in blocking solution [1% heat inactivated horse serum in 0.1% Triton-X/PBS (Sigma)] for 5 min, followed by incubation overnight at 4°C in selected primary antibodies diluted in blocking solution. The following primary antibodies were used: guinea pig anti-Lmx1b (gift from Tom Jessell, Columbia University, New York), rabbit anti-NK1R (1:1000, Sigma, S8305), rabbit anti-Lim1 (Tom Jessell), mouse anti-calcitonin gene-related peptide (CGRP, 1:1000, Abcam, ab81887), rabbit anti-Iba1 (1:500, Wako, 019–19741), rabbit anti-PKCγ (1:1000, Santa Cruz Biotechnology, sc-211), sheep and rabbit anti-GFP (1:1000, Biogenesis, 4745–1051; Invitrogen, A11122), rabbit anti-synapsin (1:1000, Millipore, AB1543P), rat anti-somatostatin (1:500, Abcam, ab30788), mouse anti-calbindin (1:1000, Sigma, C9848), and anti-cleaved-caspase3 (1:1000, Cell Signaling Technology, 9664). The antibody characteristics are described in the manufacturers' information sheets.

After the incubation in primary antibodies, samples were washed with PBS and incubated with appropriate secondary antibodies for 1 h at room temperature. The following secondary antibodies were used: Cy3-conjugated AffiniPure Donkey anti-mouse (rabbit, goat, or guinea pig) IgG (1:1000, Jackson ImmunoResearch Laboratories), AlexaFluor-488 donkey anti-mouse (rabbit, mouse, rat, or sheep) IgG (1:1000, Invitrogen). The isolectin IB4 AlexaFluor-568 conjugate (1:500, Invitrogen) was added with secondary antibodies and incubated 1 h at room temperature.

Images were acquired using a Leica DM6000 microscope or a Zeiss LSM confocal microscope with Volocity imaging software (Improvision).

Statistical analysis. Means were compared with Student's unpaired *t* tests with the threshold for statistical significance set at 0.05.

Results

Lmx1b is expressed in NK1R dorsal horn neurons

During embryonic development, Lmx1b is expressed in glutamatergic excitatory dorsal horn neurons (Cheng et al., 2004; Dai et al., 2008). To determine whether a subpopulation of Lmx1b-expressing neurons might be involved in specific nociceptive functions, we used immunohistochemical staining and examined a potential coexpression of Lmx1b and of the neurokinin-1 receptor (NK1R). NK1R is the receptor for substance P, a neuropeptide released from a subpopulation of primary nociceptors in the dorsal horn. This receptor is mainly expressed in excitatory dorsal horn neurons (Littlewood et al., 1995), including lamina I projection neurons (Mantyh et al., 1995, 1997; Doyle and Hunt, 1999; Todd et al., 2002). Coexpression of NK1R and Lmx1b was examined at E18.5, when neurons have reached their final position in the superficial spinal cord (Altman and Bayer, 1984) (Fig. 1). At this age, Lmx1b-expressing neurons are located in lamina I-IV, whereas NK1R expression is mostly confined to neurons in lamina I and IV (Fig. 1*A*) (Littlewood et al., 1995; Todd et al., 2000). High extent of coexpression of NK1R and Lmx1b was observed in lamina I neurons (66 ± 0.9% of $NK1R^+$ cells in lamina (L) I were $Lmx1b^+$), but not in lamina IV neurons (15 ± 11.3% of $NK1R^+$ neurons in LIV were $Lmx1b^+$; 16.2 ± 3.0 of 24.7 ± 4.4 $NK1R^+$ average per section LI neurons and 2.1 ± 1.7 of 13.4 ± 3.7 $NK1R^+$ LIV neurons expressed Lmx1b; $n = 3$ animals; data not shown) (Fig. 1*B*,*C*).

To determine whether the lamina I neurons coexpressing Lmx1b and NK1R were spinofugal projection neurons, we retrogradely labeled spinothalamic tract (STT) neurons by injecting the axonal tracer FG into the thalamus of newborn pups (Davidson et al., 2010b) and analyzed their spinal cords at postnatal day (P) 7. FG-labeled spinothalamic projection neurons in lamina I of the cervical spinal cord expressed Lmx1b and NK1R proteins (Fig. 1*D*–*G*). For quantitative analysis, we performed *in situ* hybridization experiments in the cervical spinal cord. These experiments showed that 77.2 ± 8.9% of the FG-labeled neurons in lamina I were expressing *Lmx1b* mRNA, whereas only 6.2 ± 3.7% of FG-labeled neurons in lamina IV-VI were expressing *Lmx1b* (average per section: 12.6 ± 3 of 16.7 ± 5 FG^+ lamina I neurons and 7.9 ± 5 of 125.5 ± 16 FG^+ lamina IV-VI neurons expressed *Lmx1b*; $n = 5$ animals; data not shown). The quantification further confirmed that the majority of STT neurons originate from deeper laminae (88%) and only a small proportion from lamina I (12%) of the spinal cord.

To further characterize Lmx1b-expressing neurons in the dorsal spinal cord, we performed co-stainings with antibodies labeling specific subpopulations of dorsal horn neurons. As previously reported, there was no overlap between Lmx1b and Lim1, a marker expressed in inhibitory interneurons of the dorsal horn (Fig. 1*J*,*M*) (Pillai et al., 2007). We found extensive colocalization between Lmx1b and somatostatin (Sst), a neuropeptide expressed by excitatory dorsal horn nociceptive neurons (Todd and Spike, 1993; Duan et al., 2014) (Fig. 1*I*,*L*). Calbindin, expressed in lamina I-III in the dorsal horn at E18.5 (Fig. 1*H*) (Ren and Ruda, 1994), was also extensively colocalizing with Lmx1b (Fig. 1*K*, arrows). Collectively, these results show that Lmx1b is expressed in the majority of excitatory dorsal horn neurons, including several subpopulations, one of them being nociceptive excitatory dorsal horn neurons that innervate the thalamus.

Lmx1b is required for the generation of excitatory dorsal horn neurons

Lmx1b is required for the normal specification of dorsal horn neurons (Ding et al., 2004). To determine a possible role of Lmx1b in nociceptive circuit development, we analyzed the dorsal spinal cord of wild-type and *Lmx1b*-null littermates by labeling specific subsets of neurons using immunohistochemical and *in situ* hybridization markers at E18.5 (Fig. 2). Expression of NK1R was completely absent from lamina I of *Lmx1b*-null spinal cords (Fig. 2*B*, arrowheads) but still present in deeper laminae. Calbindin-expressing cells, normally present in lamina I-III at E18.5 in wild-type mice, were significantly reduced in number in *Lmx1b*-null mice (Fig. 2*C*–*E*; average 245 ± 77 cells per section in wild-type dorsal horn vs 78 ± 22 per section knock-out dorsal horn, $p = 0.02$, $n = 3$). The number of *Reelin*-expressing neurons in laminae I-II (Villeda et al., 2006; Akopians et al., 2008) was reduced in the superficial laminae but appeared unchanged in deeper laminae (Fig. 2*F*–*H*, arrowheads in Fig. 2*G*; 252 ± 22 per section in wild-type vs 132 ± 47 per section in knock-out, $p = 0.02$, $n = 3$). In contrast, the number of dorsal horn neurons expressing inhibitory markers, Lim1 and *Gad1* (Erlander and Tobin, 1991; Pillai et al., 2007), was unchanged in *Lmx1b*-null animals (673 ± 41 $Gad1^+$ cells per section of wild-type dorsal horns vs 722 ± 47 cells in knock-out dorsal horns, $p = 0.25$, $n = 3$; 509 ± 82 Lim1 cells in wild-type vs 418 ± 65 cells in mutant, $p = 0.21$, $n = 3$). The distribution of inhibitory neurons was however markedly changed from a scattered to a more clustered

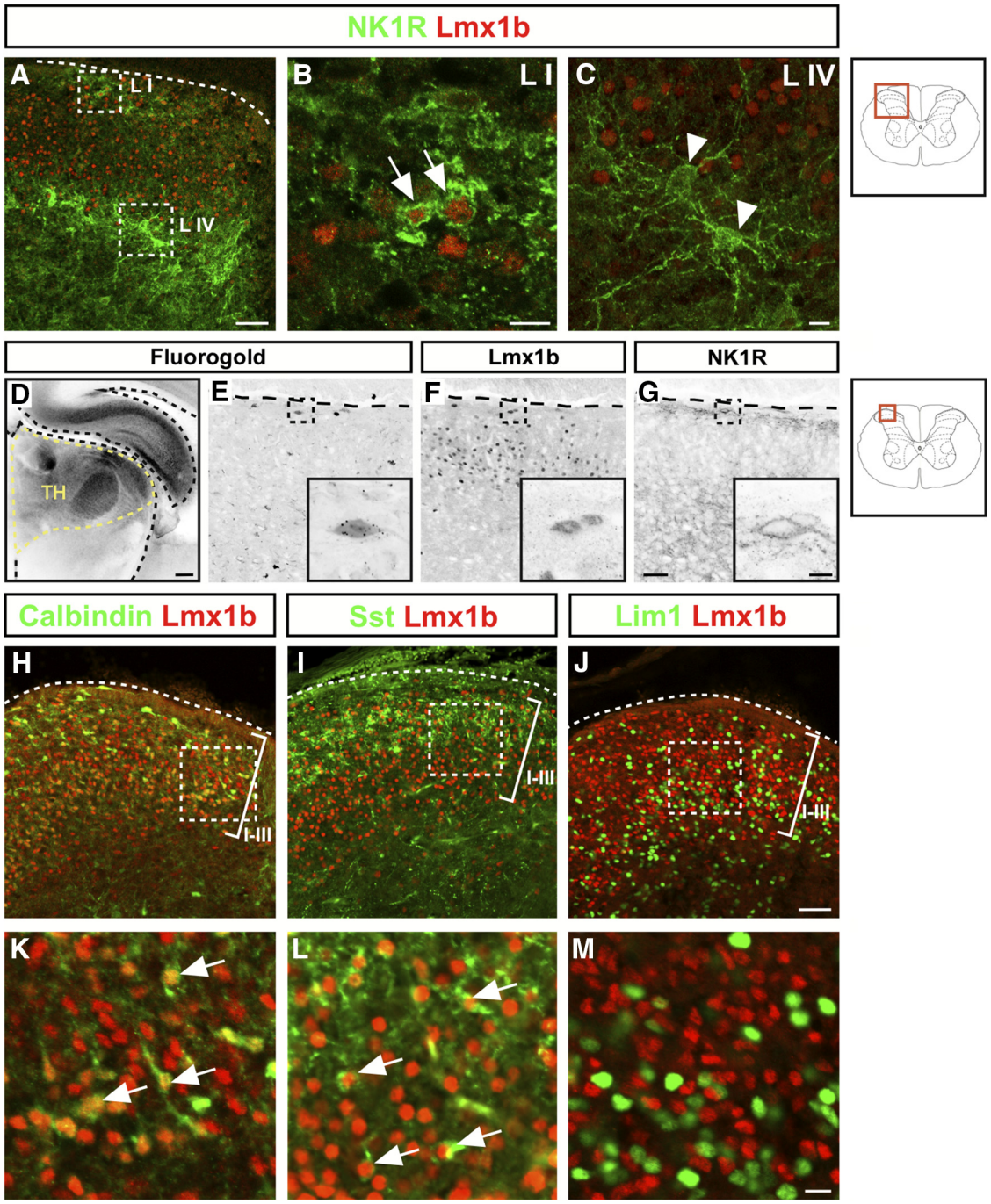

Figure 1. Lmx1b is expressed in NK1R dorsal horn neurons. ***A***, Dorsal horn of wild-type spinal cord (area of red inbox) stained with antibodies against NK1R and Lmx1b. Lmx1b is expressed in excitatory cells in lamina I-IV, whereas NK1R shows strong labeling in lamina I and lamina IV. ***B***, Inset in ***A*** showing lamina I neurons coexpressing NK1R and Lmx1b (arrows). ***C***, Inset in ***A*** of lamina IV showing NK1R-expressing neurons (arrowheads) without Lmx1b expression. ***D***, P7 brain section illustrating the thalamic injection site of FG. ***E–G***, Retrogradely labeled FG$^+$ spinothalamic tract neurons in lamina I of wild-type cervical spinal cord at P7 also express Lmx1b and NK1R. ***H***, ***K***, Calbindin is expressed in lamina I-III in the wild-type dorsal horn at E18.5 and overlaps in the majority of cells with Lmx1b expression (***K***, arrows). ***I***, ***L***, Sst and Lmx1b show overlap in dorsal horn neurons in lamina I-III (***L***, arrows). Sst is localized to the cytoplasm of the cells, whereas Lmx1b staining is nuclear. ***J***, ***M***, Lim1 is expressed in inhibitory dorsal interneurons and shows no overlap with Lmx1b expression in lamina I-IV wild-type E18.5 spinal cord. Scale bars: ***A***, ***E–G***, ***H–J***, 50 μm; ***B***, ***C***, ***E–G*** (insets), ***K–M***, 10 μm; ***D***, 200 μm.

and uneven localization (Fig. 2*I–N*; compare insets in Fig. 2*I*,*J* and Fig. 2*L*,*M*).

Because previous studies suggested that Lmx1b is not required for the normal proliferation of dorsal horn neurons (Ding et al., 2004), we reasoned that the observed loss of excitatory markers could result from a neuronal fate switch or from their decreased cellular survival. To address these possibilities, we counted the total numbers of cells in the dorsal horn of E18.5 wild-type and *Lmx1b* mutant embryos. The total number of cells in the cervical dorsal horn, assessed by DAPI staining, was decreased by 736 ± 338 cells in the mutant spinal cord at cervical level (2427 ± 125 DAPI$^+$ nuclei in wild-type dorsal horn vs 1500 ± 33 DAPI$^+$ nuclei in knock-out dorsal horn, $p < 0.01$, $n = 3$) arguing that Lmx1b is required for neuronal survival. Indeed, staining for the apoptotic marker cleaved Caspase3 (Casp3) in E18.5 spinal cord sections showed a significant increase in the number of Casp3$^+$

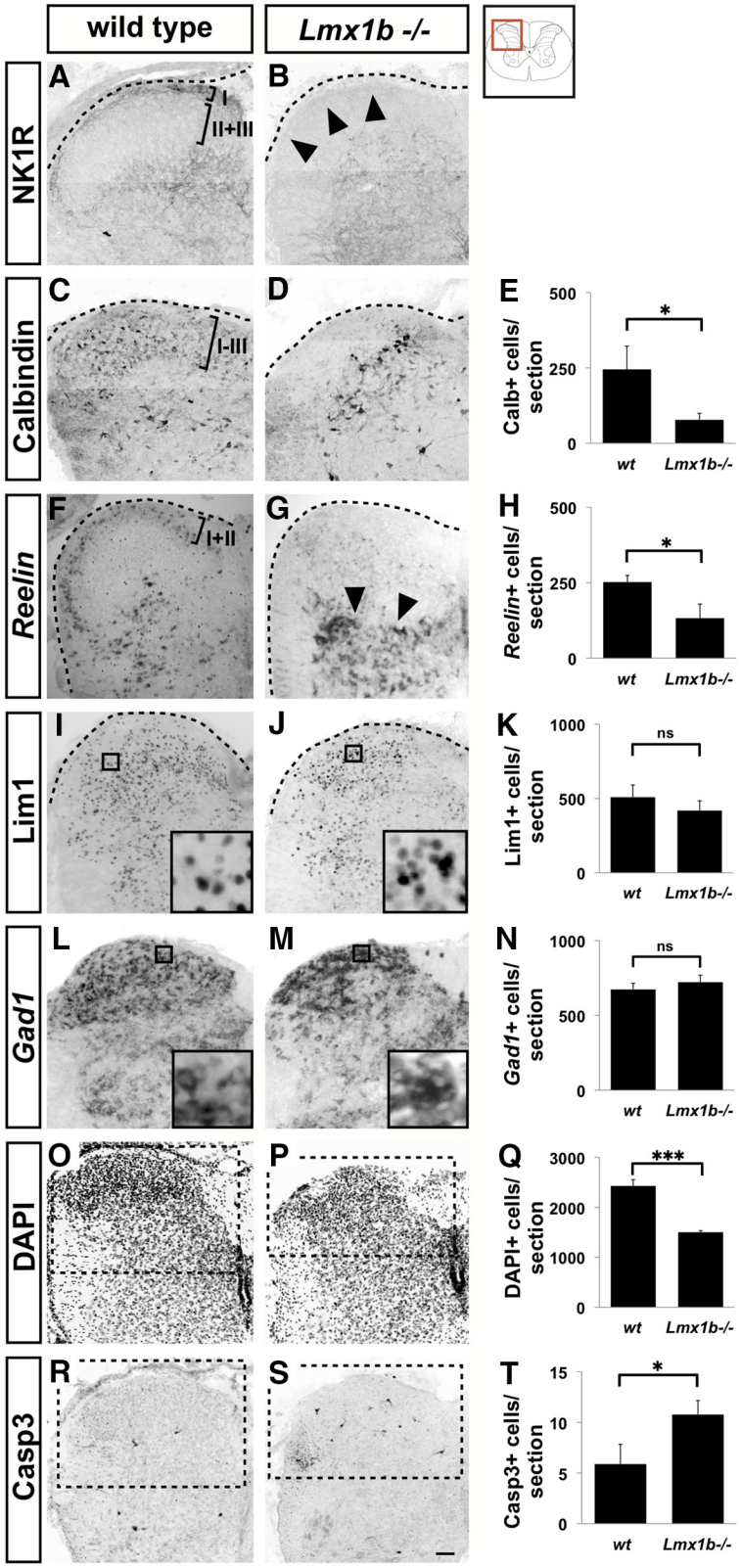

Figure 2. Lmx1b is required for the generation of excitatory dorsal horn neurons. All panels represent cervical spinal cord sections at E18.5. ***A***, ***B***, NK1R immunodetection in wild-type (***A***) and *Lmx1b* knock-out (***B***) cervical spinal cord. NK1R is strongly expressed in wild-type lamina I but absent in the most superficial laminae of $Lmx1b^{-/-}$ mice (arrowheads). ***C–E***, Calbindin protein is expressed in many cells in lamina I-III and lamina V in wild-type dorsal horn (***C***) but is absent in the most superficial laminae in $Lmx1b^{-/-}$ mice (***D***). Quantification of $Calb^{+}$ cells in dorsal horn (area of quantified cells as in inbox ***O*** and ***P*** for wild-type and $Lmx1b^{-/-}$) shows a significant reduction in $Lmx1b^{-/-}$ mice (245 ± 77 in wild-type dorsal horn vs 78 ± 22 knock-out dorsal horn, $p = 0.02$, $n = 3$). ***F–H***, *Reelin* mRNA detection in wild-type dorsal horn in lamina I-II and deeper laminae (***F***). The number of *reelin*-expressing cells in $Lmx1b^{-/-}$ superficial dorsal horn is significantly reduced, whereas in deeper laminae cells in the dorsal horn of *Lmx1b*-null embryos (5.9 ± 2 $Casp3^{+}$ cells/section in wild-type vs 10.8 ± 1.4 $Casp3^{+}$ cells/section in knock-out, $p = 0.02$, $n = 3$). Because the total number of Lmx1b-expressing cells in the E18.5 dorsal horn of a cervical section of wild-type mice (Fig. 4*C*; 357 ± 44; $n = 3$; $p = 0.09$) is smaller than the number of missing cells in the knock-out, *Lmx1b* mutation could have a non–cell-autonomous effect on dorsal horn neuron survival. Alternatively, it is possible that the number of $Lmx1b^{+}$ cells at E18.5 is an underestimation of all cells that have expressed Lmx1b at earlier stages, and the requirement of Lmx1b for survival is cell-autonomous. In summary, our data show that Lmx1b is required for the normal development and survival of glutamatergic neurons in the superficial laminae of the dorsal spinal cord.

The intersection of Hoxb8 and Lmx1b defines a subpopulation of excitatory dorsal horn neurons

Lmx1b knock-out animals die perinatally with kidney defects (Chen et al., 1998). To assess the functional consequences of the loss of Lmx1b glutamatergic neurons in the spinal cord on nociception, we generated an *Lmx1b* conditional mutant mouse line using a brain-sparing Cre driver mouse line. The *Hoxb8::Cre* line expresses Cre recombinase in the spinal cord and DRG neurons caudal of cervical level C5 but largely spares the brain (Witschi et al., 2010). Furthermore, *Hoxb8* shows strong expression in the dorsal spinal cord during development and at E18.5 overlaps with the *Lmx1b* expression domain in lamina I-IV (Fig. 3*E*,*F*) and is maintained

←

it is unchanged (***G***, arrowheads, 252 ± 22 in wild-type vs 132 ± 47 in knock-out, $p = 0.02$, $n = 3$). ***I–N***, Number of inhibitory cells as detected by Lim1 protein (***I–K***, 509 ± 82 Lim1 cells in wild-type vs 418 ± 65 cells in mutant, $p = 0.21$, $n = 3$) and *Gad1* mRNA (***L–N***, 673 ± 41 $Gad1^{+}$ cells per section of wild-type dorsal horns vs 722 ± 47 cells in mutant dorsal horns, $p = 0.25$, $n = 3$) is not different between wild-type and *Lmx1b* mutants. These cells, however, are more clustered in $Lmx1b^{-/-}$ dorsal horn (compare insets in wild-type, ***I***, ***L***, with insets in $Lmx1b^{-/-}$, ***J***, ***M***). ***O–Q***, Quantification of DAPI-stained cells in dorsal horn (marked area in ***O***, ***P***, comprises lamina I-V) shows a significant decrease in the total number of cells in the dorsal horn of $Lmx1b^{-/-}$ mice (2427 ± 125 $DAPI^{+}$ nuclei in wild-type dorsal horn vs 1500 ± 33 $DAPI^{+}$ nuclei in knock-out dorsal horn, $p = 0.0002$, $n = 3$). ***R–T***, Cleaved-caspase 3 staining shows a significant increase in the number of apoptotic cells in $Lmx1b^{-/-}$ dorsal horn at E18.5 compared with wild-type (5.9 ± 2 $Casp3^{+}$ cells/section in wild-type vs 10.8 ± 1.4 $Casp3^{+}$ cells/section in knock-out, $p = 0.02$, $n = 3$). Error bars indicate ± SD. Scale bar, 50 μm. $^{*}p < 0.05$; $^{***}p < 0.001$; ns, Not significant.

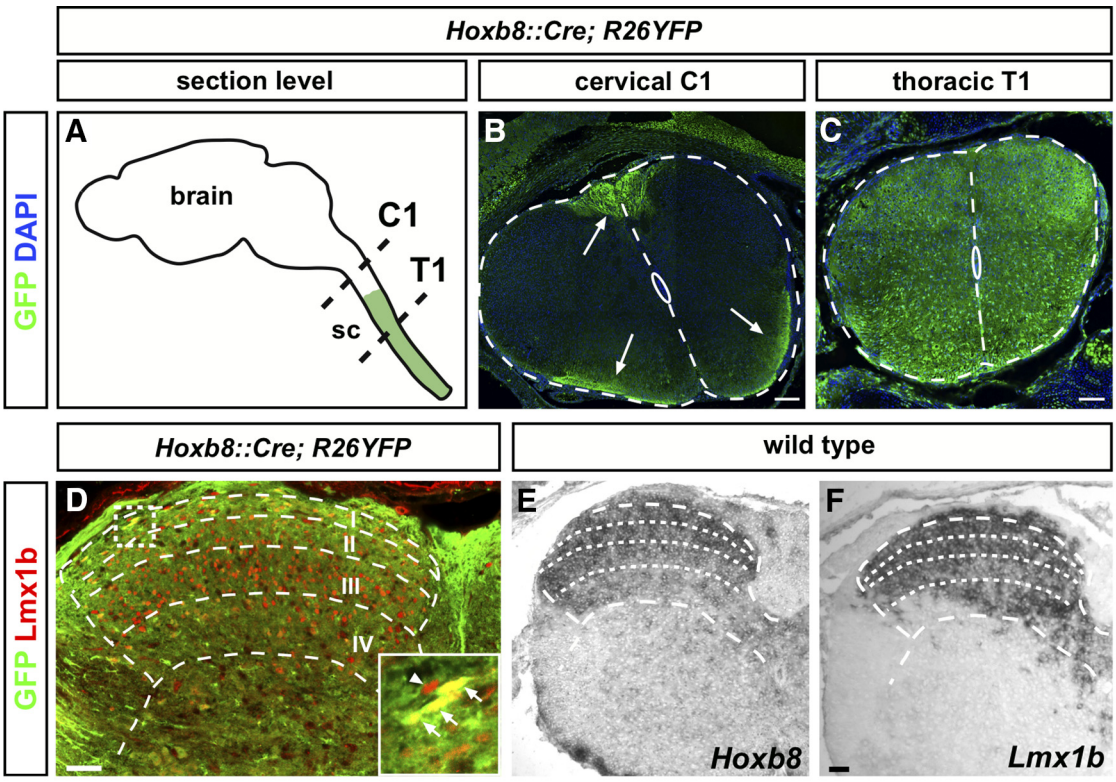

Figure 3. Characterization of the brain-sparing *Hoxb8::Cre* line. ***A***, Schematic illustration of spinal cord specific GFP expression caudal to cervical level C5 in *Hoxb8::Cre* mice harboring the Cre recombinase reporter *R26YFP*. ***B***, GFP immunostaining at cervical level C1 shows no GFP $^+$ cell bodies but projections in the lateral and ventral funiculus and dorsal column (arrows). ***C***, At the thoracic level, many cell bodies in the dorsal and ventral horn and projections in the white matter of the spinal cord are GFP $^+$. ***D***, Colabeling of GFP and Lmx1b protein in P0 *Hoxb8::Cre; R26YFP* spinal cord dorsal horn at cervical level C7. Many cells coexpress GFP and Lmx1b (arrows in inset), and some show no colabeling (arrowhead in inset). ***E***, ***F***, Detection of *Hoxb8* and *Lmx1b* mRNA in E18.5 cervical spinal cord. At this age, their expression domains are very similar in lamina I-IV. Scale bars: ***B***, ***C***, 100 μm; ***D–F***, 50 μm.

in *Lmx1b* knock-outs (Ding et al., 2004). To assess Cre expression, we crossed the *Hoxb8::Cre* line to the reporter *Rosa26YFP*, which activates YFP expression in all cells that have expressed the Cre recombinase. At P0, we observed many GFP-positive cells in the dorsal and ventral spinal cord caudal of cervical level C5 (Fig. 3*A–C*) and many cells coexpressing Lmx1b and GFP in the dorsal horn (Fig. 3*D*). Thus, using this Cre line enabled us to delete *Lmx1b* expression in the spinal cord while leaving *Lmx1b* expression in the hindbrain, midbrain, and forebrain largely intact (Dai et al., 2008). In E18.5 conditional *Hoxb8::Cre; Lmx1b$^{fl/fl}$* mutants (*Lmx1b^{CND}*), at cervical levels more rostral than C5, we did not observe any obvious changes in Lmx1b expression (data not shown). However, in the same animals, at cervical levels more caudal than C5, compared with *Lmx1b$^{+/fl}$* or *Lmx1b$^{fl/fl}$* controls (*Lmx1b^{CTL}*), we observed a loss of ~40% of Lmx1b neurons in the dorsal spinal cord, suggesting that *Hoxb8::Cre* drives Cre expression in ~40% of Lmx1b cells (323 ± 21 Lmx1b$^+$ cells in *Lmx1b^{CTL}* vs 183 ± 43 Lmx1b$^+$ cells in *Lmx1b^{CND}* mice, $p = 0.007$, $n = 3$; Fig. 4*C–E*).

To further characterize the dorsal horn subpopulations affected in *Lmx1b^{CND}* embryos, we performed *in situ* hybridization and immunohistochemistry for dorsal horn markers, including those of excitatory and inhibitory neurons. NK1R expression was reduced in the most superficial lamina in the conditional mutant (Fig. 4*F*, *G*). Also, *reelin*-expressing neurons in lamina I and II (Villeda et al., 2006; Akopians et al., 2008) were fewer in numbers in the *Lmx1b^{CND}* spinal cord (122 ± 24 *reelin*$^+$ cells in *Lmx1b^{CTL}* lamina I-III vs 28 ± 11 *reelin*$^+$ cells in *Lmx1b^{CND}* lamina I-III, $p = 0.003$, $n = 3$) (Fig. 4*H–J*). *Somatostatin*-expressing neurons were also significantly decreased in number in the dorsal horn of *Lmx1b^{CND}* mice (Fig. 4*K–M*) (77 ± 10 *Sst*$^+$ cells/section in *Lmx1b^{CTL}* vs 31.6 ± 5 *Sst*$^+$ cells/section in *Lmx1b^{CND}*, $p = 0.002$, $n = 3$), whereas the number of inhibitory neurons, labeled by the transcription factor Lim1, was unchanged (Fig. 4*N–P*; 264 ± 21 Lim1$^+$ cells/section in *Lmx1b^{CTL}* lamina I-III vs 269 ± 80 cells/section in the *Lmx1b^{CND}* lamina I-III, $p = 0.92$, $n = 3$).

In summary, compared with the *Lmx1b*-null mutant, the *Lmx1b^{CND}* mutants show a more subtle reduction in the number of Lmx1b neurons and of excitatory cells, including NK1R-, *reelin*-, and *somatostatin*-expressing neurons, in the dorsal horn without any apparent effect on the number of inhibitory neurons. The intersection of *Lmx1b*- and *Hoxb8*-driven Cre expression in the dorsal horn thus defines a subpopulation of Lmx1b-expressing excitatory cells.

Reduced innervation of nociceptive brain structures in *Lmx1b^{CND}*

The majority of projection neurons (~80%) in lamina I of the dorsal horn express NK1R (Li et al., 1996, 1998; Todd et al., 1998, 2000) and innervate several brain regions, including the thalamus, the PAG, and the Pb (Cechetto et al., 1985; Hylden et al., 1989; Burstein et al., 1990; Al-Khater et al., 2008). Because the number of NK1R-expressing neurons in lamina I was reduced in *Lmx1b^{CND}* mutants, we asked whether this led to a decreased innervation of the thalamus, PAG, and/or Pb. To label supraspinal axon projections, we introduced the *Lmx1b^{CND}* mutation into the background of the *Rosa26:lox:tdTomato:lox:GFP (R26mGFP)* transgene, which induces the expression of a membrane-targeted

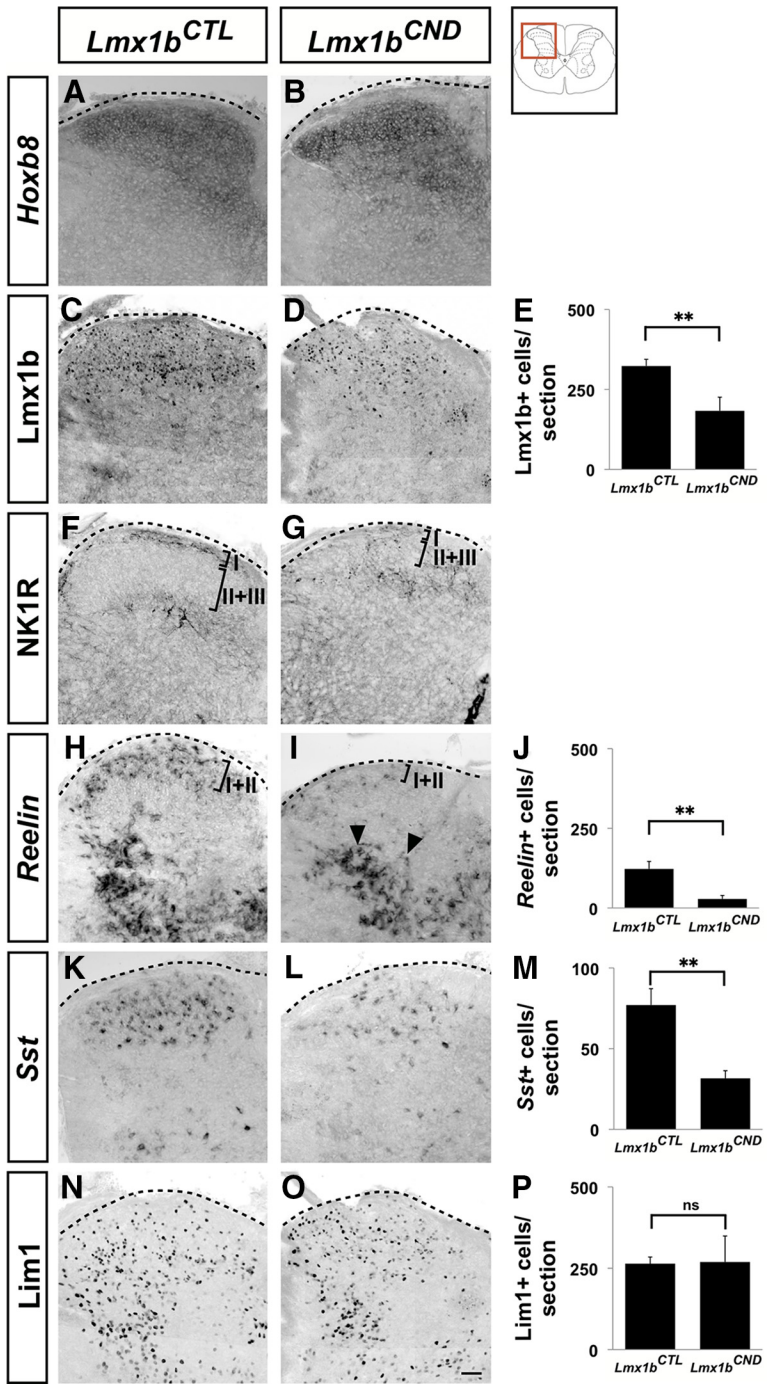

Figure 4. Loss of specific neuronal populations in *Lmx1b*^{CND} mutants. All panels represent cervical spinal cord sections caudal to level C5 at E18.5. ***A***, ***B***, Detection of *Hoxb8* mRNA in E18.5 spinal cord at cervical level C7 shows expression in dorsal horn of *Lmx1b*^{CTL} and *Lmx1b*^{CND} mice. ***C–E***, Immunodetection of Lmx1b shows a ~40% reduction in the number of Lmx1b-positive cells in *Lmx1b*^{CND} at cervical level C7 (323 ± 21 Lmx1b^{+} cells in *Lmx1b*^{CTL} vs 183 ± 43 Lmx1b^{+} cells in *Lmx1b*^{CND} mice, $p = 0.007$, $n = 3$). ***F***, ***G***, The number of NK1R-expressing cells is reduced in lamina I of *Lmx1b*^{CND}. The lamina I and lamina II + III domains are also reduced in *Lmx1b*^{CND}. ***H–J***, The number of cells expressing *reelin* mRNA is significantly reduced in lamina I-III in *Lmx1b*^{CND} (122 ± 24 *reelin*$^{+}$ cells in *Lmx1b*^{CTL} lamina I-III vs 28 ± 11 *reelin*$^{+}$ cells in *Lmx1b*^{CND} lamina I-III, $p = 0.003$, $n = 3$). ***K–M***, *Sst*-expressing cells also show a reduction in number in the dorsal horn of *Lmx1b*^{CND} mice (77 ± 10 *Sst*$^{+}$ cells/section in *Lmx1b*^{CTL} vs 31.6 ± 5 *Sst*$^{+}$ cells/section in *Lmx1b*^{CND}, $p = 0.002$, $n = 3$). ***N–P***, Lim1 immunodetection shows the same number of expressing cells in lamina I-III in *Lmx1b*^{CND} and in *Lmx1b*^{CTL} (264 ± 21 Lim1^{+} cells/section in *Lmx1b*^{CTL} lamina I-III vs 269 ± 80 cells/section in the *Lmx1b*^{CND} lamina I-III, $p = 0.92$, $n = 3$). Error bars indicate ±SD. Scale bar, 50 μm. **$p < 0.01$; ns, Not significant.

GFP under the control of Cre, allowing the visualization of the entire length of axonal projections and their innervation targets (Muzumdar et al., 2007). Because there is no Cre expression in the brain and in the spinal cord rostral to cervical level C4 of *Hoxb8::Cre* animals, all GFP expression in these areas is associated with axons originating from more caudal levels of the spinal cord in *Hoxb8::Cre; R26mGFP* mice (Fig. 5*A*) (Witschi et al., 2010). The C1 spinal cord at E18.5 showed strong GFP labeling in the lateral and ventral funiculi and dorsal column in *Hoxb8::Cre; R26mGFP* control and *R26mGFP; Lmx1b*^{CND} animals (Fig. 5*C*,*D*, white arrowhead, arrow, and black arrowhead, respectively), consistent with the location of spinofugal axon tracts originating in the caudal regions of the spinal cord (Giesler et al., 1981; Lima, 2009; Davidson et al., 2010a). Because Hoxb8::Cre is expressed in DRG neurons (Witschi et al., 2010), GFP-positive primary afferents are also likely to contribute to the labeling in the dorsal funiculi. At P2, we observed strong innervation of the lateral part of the ventral posterolateral nucleus (VPL) of the thalamus, the PAG, and the Pb by GFP-positive projections (Fig. 5*G*,*K*,*O*). The VPL was identified by *Sert* (Fig. 5*F*) (Yuge et al., 2011) and the Pb by *Lmx1b* expression in adjacent sections (Fig. 5*N*) (Dai et al., 2008), and the PAG by its characteristic DAPI stain pattern (Fig. 5*J*).

The lateral part of the VPL of the thalamus (Fig. 5*G*, arrowheads) is likely to be innervated by STT neurons that reside in lamina I, in lamina IV-VI, and also in deeper laminae (Davidson et al., 2010a). Axons from STT cells ascend in the ventral and lateral funiculus in a somatotopic fashion on the contralateral side of the spinal cord, with axons from lamina I cells ascending more dorsally in the lateral funiculus than axons from cells in deeper laminae of the dorsal horn (Giesler et al., 1981; Apkarian and Hodge, 1989). Because we could observe GFP-positive axons in the dorsal and ventral part of the lateral funiculus of the spinal cord at cervical level (Fig. 5*C*,*D*, white arrowhead and arrow, respectively), it is likely that they originate from STT projection neurons in superficial and also deeper laminae of the spinal cord. Furthermore, axons originating from level C5 and caudal spinal cord are ascending more laterally in the funiculus than those originating in the rostral spinal cord and innervate the lateral aspect of the VPL in a somatotopic fashion (Giesler et al., 1981; Gauriau and Bernard, 2004). The innervated lateral area in the VPL of the thalamus as shown in Figure 5*G* therefore represents the more caudal levels of the spinal cord where *Hoxb8::Cre* is expressed.

Analysis of GFP^{+} axon location in *R26mGFP; Lmx1b*^{CND} at P2 showed the same extent of VPL innervation as in control

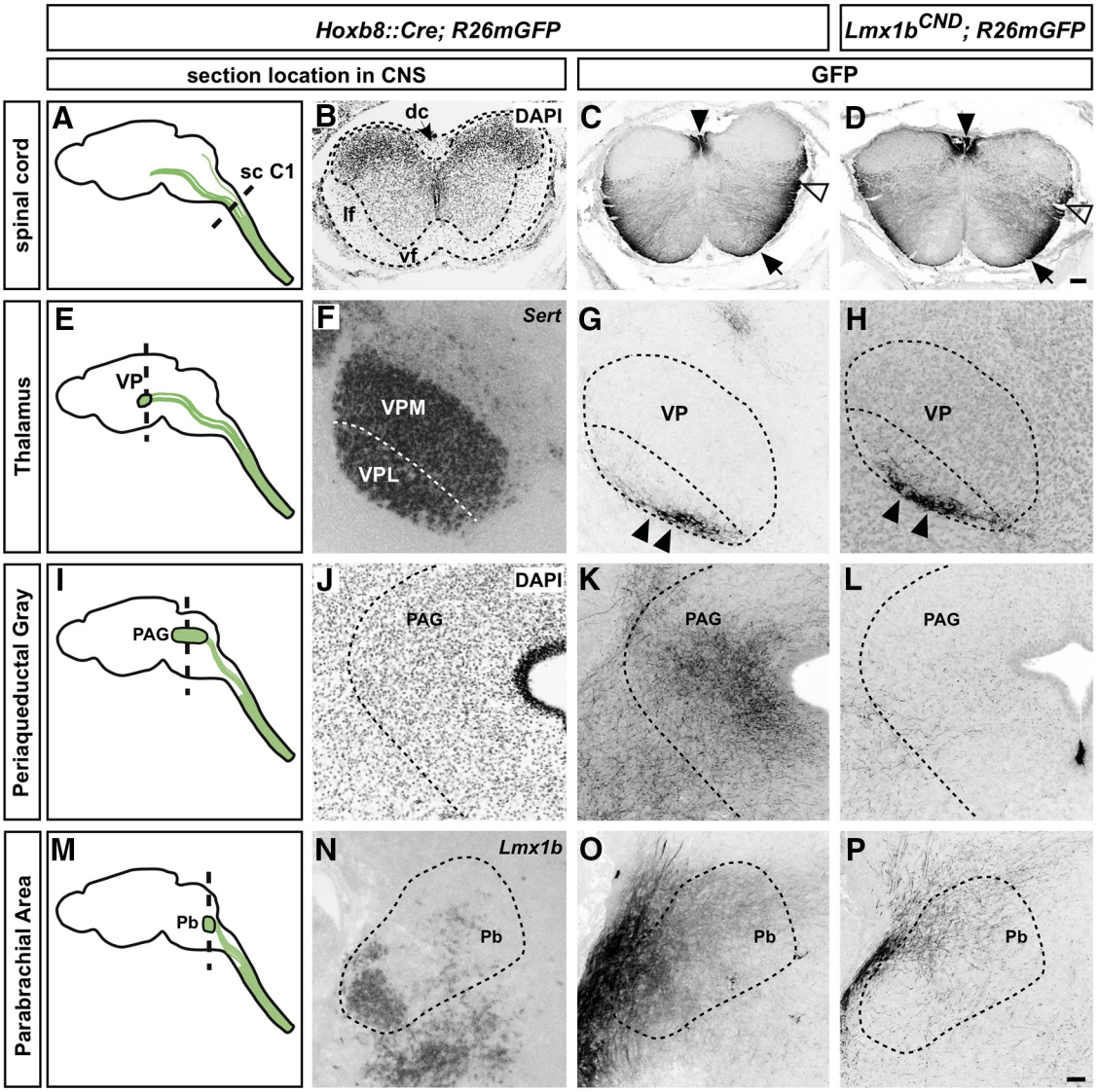

Figure 5. Reduced innervation of specific brain structures by *Hoxb8::Cre*-expressing projection neurons in *Lmx1b*^{CND} mutants. ***A–D***, Analysis of GFP expression in spinal cord at cervical level C1 in E18.5 *Hoxb8::Cre; R26mGFP* (control) and *Lmx1b*^{CND}*; R26mGFP* mice ($n = 3$). Fluorescent signal has been color-inverted such that dark areas correspond to GFP expression. Level of spinal cord (sc) analyzed is depicted in ***A*** and identified by DAPI staining (***B***). In control spinal cord, many GFP-expressing projections are labeled in the lateral (lf) and ventral funiculus (vf) (***C***, white arrowhead and arrow, respectively) and dorsal column (dc) (***C***, arrowhead) likely to originate from more caudal spinal cord levels and projecting rostrally as shown in ***A***. Immunostaining for GFP labels projections in the same areas in *Lmx1b*^{CND}*; R26mGFP* spinal cord as in control mice (***D***). ***E–H***, Analysis of innervation of the thalamus by GFP-positive projections at P2. The location of the VP is shown in ***E*** and was identified by *Sert* expression (***F***), which is expressed in the ventral posteromedial (VPM) and VPL part of the nucleus. The lateral part of the VPL is innervated by GFP-positive spinothalamic projections in control (***G***, arrowheads) and *Lmx1b*^{CND}*; R26mGFP* mice (***H***, arrowheads). ***I–L***, Innervation of the PAG was analyzed after identifying the location by its characteristic DAPI staining (***J***). GFP labeling shows strong innervation of the lateral part of the PAG in control mice (***K***) but only very few projections in *Lmx1b*^{CND}*; R26mGFP* mice (***L***). ***M–P***, The Pb, located in the hindbrain (***M***), was identified by its characteristic *Lmx1b* expression pattern (***N***). GFP staining showed strong innervation of the Pb in control mice (***O***) but severely reduced innervation in *Lmx1b*^{CND}*; R26mGFP* mice (***P***) ($n = 3$). Scale bars: ***B–D***, 100 μm; ***F–H***, ***J–L***, ***N–P***, 50 μm.

animals (Fig. 5*G*,*H*), suggesting that its origins are mostly STT neurons in deeper laminae of the dorsal horn unaffected by Lmx1b loss in *Lmx1b*^{CND} mice. Interestingly, the analysis of *Lmx1b*^{CND} midbrain and hindbrain revealed a strong reduction in innervation of PAG and Pb (Fig. 5*L*,*P*). Because most lamina I projection neurons innervate the PAG and Pb (Spike et al., 2003), this suggests that their normal development is affected in *Lmx1b*^{CND} mice and therefore that Lmx1b is required for the normal targeting of PAG and Pb.

Together, our results demonstrate that PAG and Pb, two nociceptive midbrain centers (Morgan et al., 1989; Bernard et al., 1994), show a drastically reduced innervation in *Lmx1b*^{CND} mutants. This suggests that Lmx1b is required for the development and specification of a distinct subset of projection neurons located in lamina I and for the innervation of specific supraspinal targets by these neurons.

Lmx1b expression in Hoxb8 neurons is required for mechanical and thermal nociception

The *Lmx1b*^{CND} mutants are viable after birth, and the majority of them reach adulthood, although they are apparently smaller than their normal littermates (data not shown). *Lmx1b*^{CND} mice show abnormal and shortened hindlimbs because of a partial overlap of *Hoxb8::Cre* and *Lmx1b* expression in embryonic hindlimbs and the requirement of *Lmx1b* for normal hindlimb development (Chen et al., 1998; Witschi et al., 2010). However, *Lmx1b*^{CND}

forelimbs develop normally and to further characterize them, we performed the weights test, which measures the forelimb muscle strength (Deacon, 2013), in which no significant differences between control and $Lmx1b^{CND}$ mice in their ability to lift different weights were detected (Fig. 6*A*). To assess the functional consequences of the loss of Lmx1b and Hoxb8-expressing glutamatergic neurons in the dorsal spinal cord, we performed several behavioral tests of sensitivity to thermal and mechanical stimuli. Because the forepaws and the tail of the $Lmx1b^{CND}$ mutants develop without any anatomical deficits, we tested mechanical and thermal sensitivity on the forepaw and at the tail level of $Lmx1b^{CTL}$ and $Lmx1b^{CND}$ animals. The tail withdrawal test to measure thermal sensitivity revealed a significant difference between control and conditional mice at 51°C (Fig. 6*B*) ($n = 8$ $Lmx1b^{CND}$ and $n = 16$ $Lmx1b^{CTL}$ adult mice, $p < 0.001$). We could also observe a significant increase in the withdrawal latency of the forepaw using the Hargreaves method (Fig. 6*C*) ($n = 8$ $Lmx1b^{CND}$ and $n = 20$ $Lmx1b^{CTL}$ adult mice; $p < 0.001$). However, we were able to induce the expression of the neuronal activity reporter *c-Fos* in the dorsal spinal cord using noxious thermal stimulation of the forepaw of P4 and 4-week-old $Lmx1b^{CTL}$ and $Lmx1b^{CND}$ mutant mice (Fig. 6*G*; P4 mice: $n = 4$, $p = 0.69$ for lamina I-III, 0.2 for lamina IV-VI; 4-week-old mice: $n = 3$, $p = 0.74$ for lamina I-III and $p = 0.68$ for lamina IV-VI).

The von Frey test of mechanical sensitivity revealed a very robust increase in the withdrawal threshold at the forepaw and tail level in $Lmx1b^{CND}$ compared with $Lmx1b^{CTL}$ littermates (Fig. 6*D*,*E*) ($n = 9$ $Lmx1b^{CND}$ and $n = 18$ $Lmx1b^{CTL}$ adult mice; forepaw $p < 0.001$; tail $p < 0.001$). Also, the paw pinch assay measuring the response latency after pinching the forepaws revealed a significant difference (Fig. 6*F*; $n = 5$ $Lmx1b^{CND}$ and $n = 7$ $Lmx1b^{CTL}$, $p = 0.009$).

Surprisingly, however, *c-Fos* expression after mechanical stimulation of the forepaw showed no significant difference in P4 and 4-week-old $Lmx1b^{CTL}$ and $Lmx1b^{CND}$ mutant mice (Fig. 6*H*,*I*) (P4 mice: $n = 4$, $p = 0.71$ for lamina I-III, 0.89 for lamina IV-VI; 4-week-old mice: $n = 3$, $p = 0.8$ for lamina I-III and $p = 0.9$ for lamina IV-VI).

Collectively, our behavioral data show that the loss of Lmx1b in Hoxb8-expressing neurons results in robustly lowered sensitivity to mechanical and thermal nociception, without an effect on dorsal horn neuron activity evoked by noxious stimulation measured by *c-Fos* expression.

Abnormal innervation of $Lmx1b^{CND}$ dorsal horn by nociceptive primary afferents

The nociceptive deficits observed in the $Lmx1b^{CND}$ mutants could be due to the loss of nociceptive cells in the dorsal horn and/or abnormal cutaneous sensory afferent innervation of the dorsal horn. Heat nociceptive signals are apparently relayed by transient receptor potential vanilloid-1 (TRPV1)-positive neurons, whereas mechanical nociception is relayed by Mas-related G-protein coupled receptor member D (Mrgprd)-expressing neurons in the DRG (Cavanaugh et al., 2009). The Mrgprd-positive DRG neurons correspond largely to nonpeptidergic cutaneous C-fibers that bind the isolectin IB4 and terminate in the middle part of lamina II of the dorsal horn (Zylka et al., 2005). Many TRPV1-positive neurons express CGRP, a marker for peptidergic afferents that terminate mainly in lamina I and outer lamina II. CGRP and IB4 labeling in adult $Lmx1b^{CTL}$ showed normal innervation of lamina I and II of the dorsal horn (Fig. 7*A*,*B*). Adult $Lmx1b^{CND}$ mice also showed innervation of the most superficial area of the dorsal horn by CGRP- and IB4-positive afferents (Fig. 7*D*,*E*). However, the innervation by IB4-positive fibers was not as robust as in $Lmx1b^{CTL}$ mice in lamina II. Additionally, we could detect the appearance of IB4 binding aggregates in the IB4 innervation zone (Fig. 7*E*, arrowheads). To analyze whether the $IB4^+$ aggregates were the byproduct of activated microglia, we stained them with antibodies against the microglia and macrophage marker Iba1 but could not detect significant overlap between Iba1 and IB4 in $Lmx1b^{CND}$ mice ($n = 3$, data not shown). CGRP-positive fibers appeared normal in adult $Lmx1b^{CND}$ mice (Fig. 7*D*,*E*) ($n = 3$).

Because Lmx1b is not expressed in DRG neurons (Ding et al., 2004), the abnormal innervation by IB4 fibers is likely to be a secondary effect due to the abnormal postsynaptic targets of these afferent projections. This is in line with previous observations in *Lmx1b* knock-out mice that showed delayed and disorganized innervation of the dorsal horn by primary afferents (Ding et al., 2004; Dunston et al., 2005). To characterize the neurons in the superficial laminae in the dorsal horn, we studied the expression of markers for lamina I and II at adult stages. PKCγ-positive dendrites occupy the inner lamina II of the dorsal horn, ventral to the IB4-positive innervation area of outer lamina II in $Lmx1b^{CTL}$ mice (Fig. 7*C*). In $Lmx1b^{CND}$ mice, however, we did not find a clear segregation of IB4 and PKCγ signals, suggesting a disorganization of inner and outer lamina II (Fig. 7*F*). Lamina I and outer lamina II were reduced in size so that the PKCγ-positive dendrites were now occupying a more superficial area of the dorsal horn. NK1R-positive neurons are normally populating lamina I of the dorsal horn and overlap with CGRP-positive afferent terminals (Fig. 7*G*). As we have observed at E18.5 before, the NK1R expression was essentially absent in $Lmx1b^{CND}$ mice, whereas the CGRP-expressing afferents still occupied the same area (Fig. 7*J*). To assess primary afferent innervation, we stained for synapsin I, a presynaptic protein regulating synaptic vesicle numbers (Ferreira and Rapoport, 2002). We could not detect an obvious reduction in the number of synapsin I-positive puncta in the $Lmx1b^{CND}$ dorsal horn (Fig. 7*I*,*L*), suggesting that the number of vesicles available for release at the nerve terminals in the dorsal horn is not affected (Fig. 7*H*,*I*,*K*–*M*). The quantification of the overlap of synapsin and IB4-positive puncta in the $Lmx1b^{CND}$ dorsal horn in an area with largely unaffected IB4 staining revealed no significant difference from controls, suggesting that the remaining $IB4^+$ afferents are still functional (Fig. 7*M*,*N*; $n = 3$).

Together, our data show a strong reduction of lamina I and outer lamina II termination of primary afferents in $Lmx1b^{CND}$ mutants. It is likely that this leads to an abnormal innervation of the dorsal horn by primary afferents relaying mechanical sensory information, supporting the behavioral test results. Interestingly, $CGRP^+$ primary sensory fibers appeared normal in conditional mice even though their target area is also strongly reduced.

Discussion

Our findings show that mouse Lmx1b is expressed in embryonic excitatory dorsal horn neurons, including those linked to nociception. *Lmx1b* mutations cause a loss of excitatory nociceptive neurons without any direct effects on inhibitory neurons. Furthermore, we show that *Hoxb8::Cre* labels spinofugal axons innervating brain areas involved in nociception and that these projections are decreased in $Lmx1b^{CND}$ mutants. Additionally, adult mice with an Lmx1b loss restricted to Hoxb8 neurons have nociception defects and disrupted organization of primary sensory afferent axons innervating the dorsal horn. Here, we discuss these findings in terms of the molecular cascades that specify

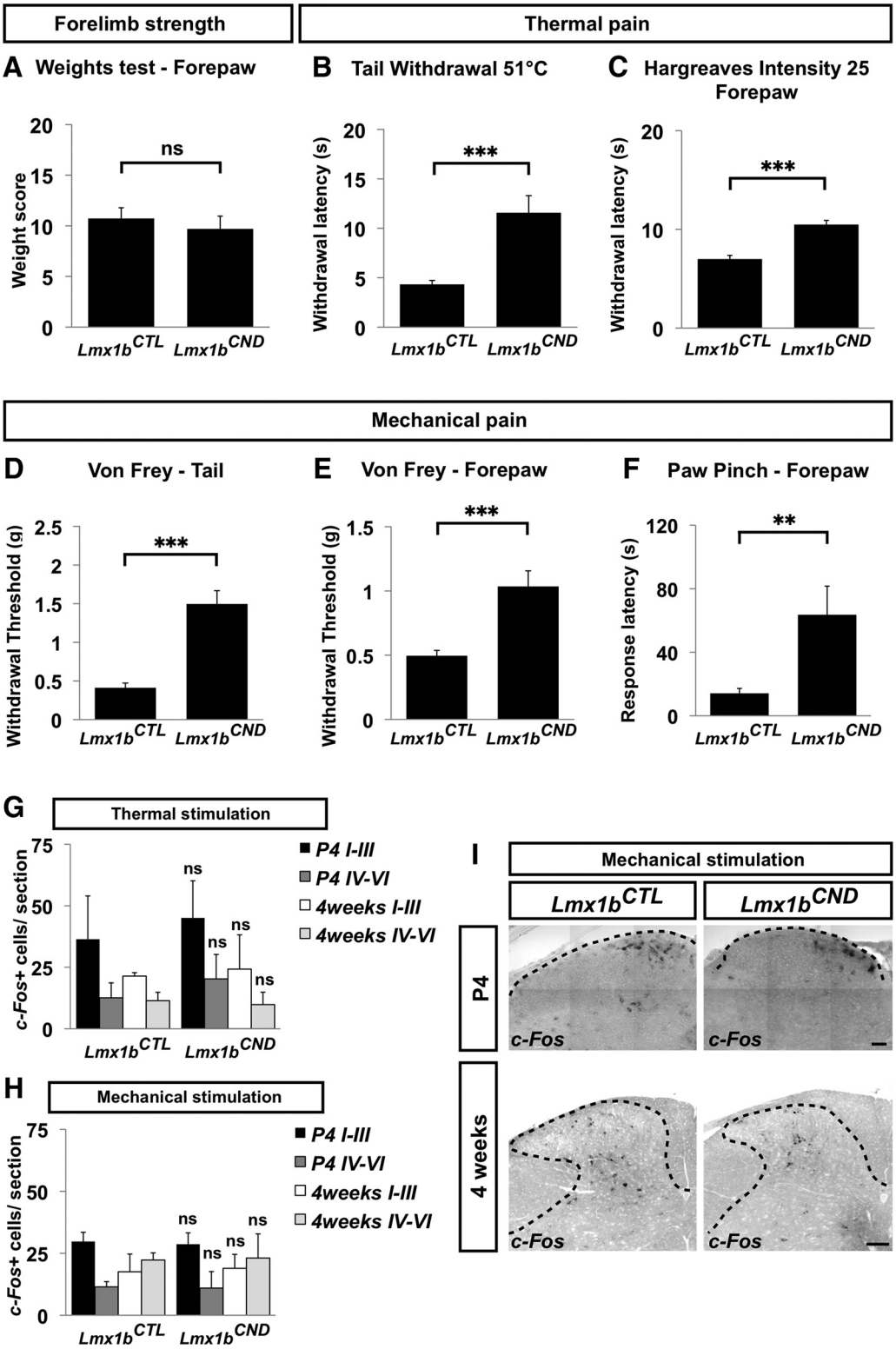

Figure 6. Lmx1b/Hoxb8 neurons in the dorsal horn are required for mechanical and thermal pain sensation. ***A***, The weights test to measure the muscle strength of the forelimbs shows no significant difference between $Lmx1b^{CND}$ and control mice ($n = 6$, $Lmx1b^{CND}$ and $n = 8$, $Lmx1b^{CTL}$; $p = 0.54$). ***B***, ***C***, Thermal sensitivity behavioral tests: the tail-withdrawal test at 51°C shows a significant difference between control and $Lmx1b^{CND}$ adult mice (***B***) ($n = 8$, $Lmx1b^{CND}$ and $n = 16$, $Lmx1b^{CTL}$; $p < 0.001$). Also, the Hargreaves test performed at the forepaws shows a significant increase in $Lmx1b^{CND}$ adult mice compared with control mice (***C***) ($n = 8$, $Lmx1b^{CND}$ and $n = 20$, $Lmx1b^{CTL}$; $p < 0.001$). ***D***, ***E***, The von Frey test of mechanical sensitivity shows significantly higher thresholds at the tail (***D***) and forepaw (***E***) level in $Lmx1b^{CND}$ mice ($n = 9$, $Lmx1b^{CND}$ and $n = 18$, $Lmx1b^{CTL}$ adult mice, forepaw, $p < 0.001$; tail, $p < 0.001$). ***F***, $Lmx1b^{CND}$ mice have a significantly longer response latency when pinched with a clip on the forepaw ($n = 5$, $Lmx1b^{CND}$ and $n = 7$, $Lmx1b^{CTL}$; $p = 0.009$). ***G***, Quantification of *c-Fos* mRNA-expressing cells in lamina I-III and lamina IV-VI of the dorsal horn at cervical level C7 in P4 and 4-week-old $Lmx1b^{CND}$ and $Lmx1b^{CTL}$ after noxious thermal stimulation of the forepaw. There are no significant differences in the number of *c-Fos*-expressing cells in the dorsal horn at these two ages (P4: 36.4 ± 17.6 *c-Fos* $^+$ cells in lamina I-III in $Lmx1b^{CTL}$ vs 45.1 ± 15 in $Lmx1b^{CND}$, $p = 0.685$; 12.6 ± 6.1 *c-Fos* $^+$ cells in lamina IV-VI in $Lmx1b^{CTL}$ vs 20.3 ± 10 in $Lmx1b^{CND}$, $p = 0.197$, $n = 4$; 4 weeks: 21.4 ± 1.4 *c-Fos* $^+$ cells in lamina I-III in $Lmx1b^{CTL}$ vs 24.3 ± 14 in $Lmx1b^{CND}$, $p = 0.74$; 11.4 ± 3.4 *c-Fos* $^+$ cells in lamina IV-VI in $Lmx1b^{CTL}$ vs 9.8 ± 5 in $Lmx1b^{CND}$, $p = 0.68$, $n = 3$). ***H***, Quantification of the number of *c-Fos*-expressing cells in the dorsal horn at cervical level C7 after noxious (*Figure legend continues.*)

spinal dorsal horn neuron development, and the molecular correlates of anatomical features of spinofugal projections and nociceptive circuits.

Lmx1b and the development of excitatory spinal dorsal horn neurons

Lmx1b has been shown to be required for the expression of specific postmitotic dorsal horn neuronal markers (Ding et al., 2004), but its requirement for the balance between inhibitory and excitatory neuron development is unclear. Within the trigeminal system, Lmx1b has been proposed to act as a switch between excitatory and inhibitory neurotransmitter identity. In *Lmx1b*-deficient mice, Xiang et al. (2012) reported an increase in the number of inhibitory neurons, with a concomitant decrease in excitatory neuron numbers and an overall decrease in total neuron numbers. In contrast to these observations, our experiments show that, in the spinal cord, Lmx1b loss does not result in increased inhibitory neuron numbers. Rather, Lmx1b is apparently important for the survival of excitatory neurons. Thus, once the excitatory neuron fate is established through the action of selector transcription factors, such as Tlx1 and Tlx3 (Cheng et al., 2004, 2005), Lmx1b could be important for its maintenance in a manner similar to Lhx1 and Lhx5 function in inhibitory neurons, with the significant difference that these transcription factors are not required for inhibitory neuron survival (Pillai et al., 2007). How Lmx1b promotes neuronal survival remains unclear. In the principal trigeminal nucleus, neuronal apoptosis caused by Lmx1b loss can be prevented by deletion of the proapoptotic protein Bax, suggesting that Lmx1b prevents apoptosis of excitatory neurons (Xiang et al., 2010). A similar requirement of Lmx1b for neuronal survival exists also for serotonergic midbrain neurons (Zhao et al., 2006).

The neuronal loss observed in *Lmx1b* mutants is reminiscent of two other mouse mutants with dorsal horn phenotypes, raising the question about their epistatic relationship. In *Prrxl1/Drg11* mutants, a decrease in total dorsal horn neuron numbers occurs without any change in early Lmx1b expression, in line with *Drg11* being genetically downstream of *Lmx1b* (Chen et al., 2001; Rebelo et al., 2010). Hoxb8 loss leads to 35% fewer neurons populating the superficial laminae but without an obvious loss of Drg11 expression (Holstege et al., 2008). Because Lmx1b controls Drg11 expression, Hoxb8 is unlikely to be required for Lmx1b expression given that its loss would have resulted in the loss of Drg11 expression. Furthermore, because our studies and past experiments argue that Lmx1b is not required for Hoxb8 expression (Ding et al., 2004), *Hoxb8* and *Lmx1b/Drg11* genetic cascades are probably not overlapping. The fact that we see a loss of excitatory neurons without an effect on inhibitory neuron markers suggests that the neuronal survival effects of Lmx1b mutation occur in a cell-autonomous manner. However, the loss of Lmx1b neurons is not without a consequence on the overall structure of the dorsal horn: in *Lmx1b*-null or $Lmx1b^{CND}$, inhibitory neurons are generated in normal numbers, but their position is altered. This appears to be an early event, preceding any loss of Lmx1b excitatory neurons, and could be the result of loss of Reelin that is normally required for dorsal horn lamination (Wang et al., 2012).

In addition to defining excitatory neurons, our Lmx1b expression profiling experiments also show that Lmx1b can be used to subdivide spinothalamic (STT) projection neurons according to their lamina of origin. Our retrograde labeling experiments argue that STT neurons in the superficial laminae are mainly Lmx1b-expressing, whereas STT neurons located in deeper laminae seldom express Lmx1b, providing a molecular subdivision of different classes of STT projection neurons. On the other hand, because both populations target the thalamus, Lmx1b is unlikely to be the general determinant of spinothalamic connectivity.

Molecular correlates and transcriptional control of spinofugal connectivity

Our studies of *Hoxb8::Cre* expression also provide the evidence that it is a general molecular label of spinal nociceptive projections. A great wealth of anatomical data describe the target structures of these neurons (Basbaum and Bushnell, 2008), but their molecular characterization has remained elusive. The *Hoxb8::Cre* line complements the Hoxa2- and Krox20-based Cre drivers labeling the analogous projections from the trigeminal nuclei to the ventral posterior nucleus (VP) and posterior nucleus (Po) thalamus (Pasqualetti et al., 2002; Oury et al., 2006). Our present study identified *Hoxb8::Cre* axons in the VPL thalamus, the PAG, and the Pb, which very likely originate from the spinal cord. Even though the *Hoxb8::Cre* line drives Cre expression also in the trigeminal nucleus (Witschi et al., 2010), we did not observe any reporter-expressing axons in the ventral posteromedial nucleus (VPM), the VP subdivision target of trigeminal neurons. The trigeminal neurons expressing *Hoxb8::Cre* are thus unlikely to be projection neurons. The relatively restricted labeling in the VPL is in line with the somatotopic organization of the VP, where the VPM is mainly innervated by trigeminal axons (Oury et al., 2006), whereas the VPL receives innervation from spinal levels, with the cervical regions as the major source, and more caudal regions contributing few projections (Gauriau and Bernard, 2004). Thus, because the *Hoxb8::Cre* expression is restricted to levels caudal to C5, the small crescent of the VPL labeled with *Hoxb8::Cre* likely represents the caudal spinal cord, correlating with electrophysiological studies of nociceptive thalamus somatotopy (Francis et al., 2008).

In addition to providing evidence that *Hoxb8::Cre* is a molecular marker of spinofugal projections, our experiments also define Lmx1b as the first gene required for spino-parabrachial and spino-periaqueductal gray connectivity. Anterograde labeling by Gauriau and Bernard (2004) showed that lamina I projection neurons innervate mainly the VPL, whereas neurons in deeper laminae do not. These lamina I projection neurons are likely to target the VPL, PAG, and the Pb, which en route to the VPL, elaborate PAG and Pb-innervating collaterals (Al-Khater and Todd, 2009). Therefore, one possibility is that STT projections originating from lamina I are unaffected by the *Lmx1b* mutation and reach the VPL, whereas their collaterals that normally innervate the PAG and Pb are not formed. Other studies using retrograde tracer injections into the lateral thalamus, however, could identify retrogradely labeled neurons in lamina I and deeper lam-

←

(*Figure legend continued.*) mechanical stimulation of the forepaw. The difference in the number of *c-Fos*-expressing cells in the dorsal horn at P4 between $Lmx1b^{CND}$ and $Lmx1b^{CTL}$ is not significant (P4: 29.8 ± 3.7 $c\text{-}Fos^+$ cells in lamina I-III in $Lmx1b^{CTL}$ vs 28.6 ± 4.6 in $Lmx1b^{CND}$, $p = 0.71$; 11.5 ± 2.1 $c\text{-}Fos^+$ cells in lamina IV-VI in $Lmx1b^{CTL}$ vs 10.9 ± 6.7 in $Lmx1b^{CND}$, $p = 0.89$, $n = 4$; 4 weeks: 17.53 ± 7.1 $c\text{-}Fos^+$ cells in lamina I-III in $Lmx1b^{CTL}$ vs 18.93 ± 5.6 in $Lmx1b^{CND}$, $p = 0.8$; 22.3 ± 2.9 $c\text{-}Fos^+$ cells in lamina IV-VI in $Lmx1b^{CTL}$ vs 23.1 ± 9.7 in $Lmx1b^{CND}$, $p = 0.9$, $n = 3$). ***I***, *c-Fos* mRNA detection at cervical level C7 after noxious mechanical stimulation of the forepaw of P4 pups and 4-week-old $Lmx1b^{CTL}$ and $Lmc1b^{CND}$ mice. The ipsilateral side of the spinal cord has many *c-Fos* mRNA-positive cells in lamina I-III and deeper laminae IV-VI, in $Lmx1b^{CTL}$ and $Lmx1b^{CND}$, at both ages. Error bars indicate ± SEM (***A–F***) and ±SD (***G,H***). Scale bar: ***I***, P4, 50 μm; 4 weeks, 100 μm. $^{**}p < 0.01$; $^{***}p < 0.001$; ns, Not significant.

inae of the spinal cord, suggesting that deeper laminae neurons also contribute to VPL innervation (Kobayashi, 1998; Lima, 2009). Therefore, the STT projections labeled by *Hoxb8::Cre* likely originate from multiple spinal laminae, with lamina I projections contributing a relatively small proportion, as revealed by retrograde labeling (Davidson et al., 2010a). Thus, the most likely explanation for the lack of effect of *Lmx1b* mutation on VPL innervation is that the majority of the STT projections, as labeled by *Hoxb8::Cre*, originate from deeper spinal laminae, which contain wide dynamic range projection neurons and are unaffected by the loss of Lmx1b. It is very likely that STT projections originating from lamina I are affected in $Lmx1b^{CND}$ mice because Lmx1b is required for neuronal viability; however, we are not able to detect their absence in the VPL because they contribute only few projections.

Hoxb8 and Lmx1b intersection genetically defines normal nociception

Genetic dissection of nociception is providing a molecular dimension to our understanding of nociceptive circuit function, with increasing specificity, for example, in terms of nociceptive modalities. *TR4* mutant mice show normal reflex responses to noxious heat but a loss of mechanical noxious stimuli-evoked pain behaviors (Wang et al., 2013), similar to a recent study inactivating Sst-expressing neurons (Duan et al., 2014). The $Lmx1b^{CND}$ mice also show an apparent loss of Sst neurons but, in addition to mechanical nociception deficits, also show diminished thermal nociception in line with a loss of other neuronal populations in addition to those expressing Sst. This is consistent with *Tlx3* conditional knock-out mice, in which *Tlx3* was deleted in lamina I and II neurons and show reduced sensitivity to noxious thermal and mechanical stimuli (Xu et al., 2013). Surprisingly, we did not observe a decrease in mechanical or thermal noxious stimulus-evoked *c-Fos* expression in $Lmx1b^{CND}$ mutants. Rather, in such mutants, we found the same number of $c\text{-}Fos^{+}$ dorsal horn neurons as in control animals. Given the disrupted dorsal horn termination of mechanical nociceptive afferents in $Lmx1b^{CND}$ mutants, one possibility is that these afferents now innervate inappropriate dorsal horn neuron targets, making them responsive to noxious stimuli and turning on *c-Fos* expression, but failing to elicit appropriate nocifensive behaviors because the activated neurons are not wired into appropriate dorsal horn circuits. Another possibility is that a lowered intensity of noxious

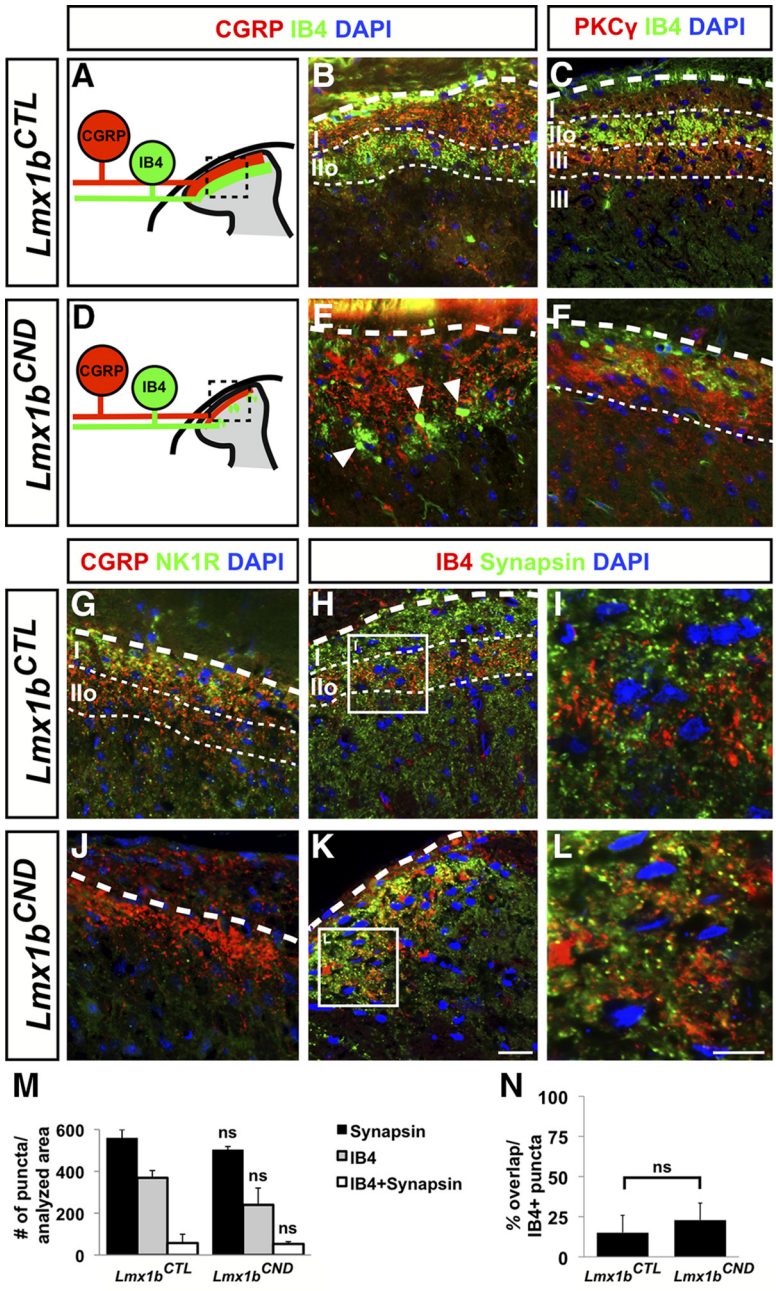

Figure 7. Abnormal innervation of dorsal horn by primary afferents that are required for mechanical sensation. ***A***, ***D***, Schematic illustration of the innervation of the dorsal horn by CGRP-positive primary afferents (red) that relay thermal sensation and IB4-positive afferents (green) relaying mechanical pain sensation. ***B***, ***E***, Stainings with an antibody against CGRP and with the isolectin IB4 in adult $Lmxb^{CTL}$ (***B***) and $Lmx1b^{CND}$ (***E***) spinal cord at cervical level C7, area of dorsal horn as in ***A***, ***D*** (inbox). CGRP-positive fibers innervate lamina I and outer lamina II in $Lmx1b^{CTL}$ and $Lmx1b^{CND}$ mice. IB4-positive afferents innervate the outer lamina II in $Lmx1b^{CTL}$ spinal cord (***B***). In $Lmx1b^{CND}$ mice, however, the innervated area in the dorsal horn is not as dense and shows IB4-positive aggregates (***E***, arrowheads). ***C***, ***F***, Labeling of PKCγ and IB4 in adult $Lmx1b^{CTL}$ (***C***) spinal cord at cervical level C7 labels PKCγ-positive cells in inner lamina II of the dorsal horn. In $Lmx1b^{CND}$ dorsal horn, the expression area of PKCγ and the termination area of IB4-positive afferents overlap and occupy a more superficial area of the dorsal horn (***F***). ***G***, ***J***, Immunostaining with antibodies against CGRP and NK1R shows innervation of NK1R-expressing neurons in lamina I of the dorsal horn by CGRP-expressing primary afferents in $Lmx1b^{CTL}$ mice (***G***). $Lmx1b^{CND}$ mice show normal innervation of the dorsal horn by CGRP-expressing afferents but absence of NK1R-expressing cells in the most superficial lamina (***J***). ***H–L***, Immunodetection of synapsin and staining with IB4 at cervical level C7 in adult $Lmx1b^{CTL}$ and $Lmx1b^{CND}$ mice. The synaptic protein synapsin labels many synapses in the innervation area of IB4-positive afferents in the dorsal horn of both $Lmx1b^{CTL}$ and $Lmx1b^{CND}$ mice. ***M***, ***N***, Quantification of synapsin $^{+}$ and IB4 $^{+}$ puncta in the innervation area of IB4-positive afferents, assessed in an area of the size shown in ***I*** and ***L*** in the dorsal horn, shows no significant difference between $Lmx1b^{CTL}$ and $Lmx1b^{CDN}$ mice. Also, the overlap of synapsin and IB4-positive puncta is unchanged in the analyzed area (557.5 $\pm$ 41.8 synapsin $^{+}$ puncta in analyzed area in $Lmx1b^{CTL}$ vs 501.3 $\pm$ 17.5 in $Lmx1b^{CND}$, $p = 0.1$; 369 $\pm$ 34.8 IB4 $^{+}$ puncta in $Lmx1b^{CTL}$ vs 239.9 $\pm$ 80.3 in $Lmx1b^{CND}$, $p = 0.06$; 57.2 $\pm$ 42.1 synapsin $^{+}$/IB4 $^{+}$ puncta in $Lmx1b^{CTL}$ vs 53 $\pm$ 10.7 in $Lmx1b^{CND}$, $p = 0.88$; $n = 3$). Scale bars: ***B***, ***C***, ***E–H***, ***J***, ***K***, 20 μm; ***I***, ***L***, 10 μm. ns, Not significant.

stimulation might reveal significant c-Fos expression induction differences between $Lmx1b^{CND}$ and control animals. A genetic intersectional approach where Lmx1b/Hoxb8-expressing neurons are inactivated without affecting their development would certainly clarify some of these questions.

References

Akopians AL, Babayan AH, Beffert U, Herz J, Basbaum AI, Phelps PE (2008) Contribution of the Reelin signaling pathways to nociceptive processing. Eur J Neurosci 27:523–537. CrossRef Medline

Al-Khater KM, Todd AJ (2009) Collateral projections of neurons in laminae I, III, and IV of rat spinal cord to thalamus, periaqueductal gray matter, and lateral parabrachial area. J Comp Neurol 515:629–646. CrossRef Medline

Al-Khater KM, Kerr R, Todd AJ (2008) A quantitative study of spinothalamic neurons in laminae I, III, and IV in lumbar and cervical segments of the rat spinal cord. J Comp Neurol 511:1–18. CrossRef Medline

Altman J, Bayer SA (1984) The development of the rat spinal cord. Adv Anat Embryol Cell Biol 85:1–164. CrossRef Medline

Apkarian AV, Hodge CJ (1989) Primate spinothalamic pathways: II. The cells of origin of the dorsolateral and ventral spinothalamic pathways. J Comp Neurol 288:474–492. CrossRef Medline

Basbaum AI, Bushnell MC (2008) Science of pain. Boston: Elsevier.

Basbaum AI, Bautista DM, Scherrer G, Julius D (2009) Cellular and molecular mechanisms of pain. Cell 139:267–284. CrossRef Medline

Bautista DM, Siemens J, Glazer JM, Tsuruda PR, Basbaum AI, Stucky CL, Jordt SE, Julius D (2007) The menthol receptor TRPM8 is the principal detector of environmental cold. Nature 448:204–208. CrossRef Medline

Ben-Bassat J, Peretz E, Sulman FG (1959) Analgesimetry and ranking of analgesic drugs by the receptacle method. Arch Int Pharmacodyn Ther 122:434–447. Medline

Bernard JF, Huang GF, Besson JM (1994) The parabrachial area: electrophysiological evidence for an involvement in visceral nociceptive processes. J Neurophysiol 71:1646–1660. Medline

Borodinsky LN, Root CM, Cronin JA, Sann SB, Gu X, Spitzer NC (2004) Activity-dependent homeostatic specification of transmitter expression in embryonic neurons. Nature 429:523–530. CrossRef Medline

Braz JM, Nassar MA, Wood JN, Basbaum AI (2005) Parallel "pain" pathways arise from subpopulations of primary afferent nociceptor. Neuron 47:787–793. CrossRef Medline

Burstein R, Dado RJ, Giesler GJ Jr (1990) The cells of origin of the spinothalamic tract of the rat: a quantitative reexamination. Brain Res 511:329–337. CrossRef Medline

Caterina MJ, Schumacher MA, Tominaga M, Rosen TA, Levine JD, Julius D (1997) The capsaicin receptor: a heat-activated ion channel in the pain pathway. Nature 389:816–824. CrossRef Medline

Cavanaugh DJ, Lee H, Lo L, Shields SD, Zylka MJ, Basbaum AI, Anderson DJ (2009) Distinct subsets of unmyelinated primary sensory fibers mediate behavioral responses to noxious thermal and mechanical stimuli. Proc Natl Acad Sci U S A 106:9075–9080. CrossRef Medline

Cechetto DF, Standaert DG, Saper CB (1985) Spinal and trigeminal dorsal horn projections to the parabrachial nucleus in the rat. J Comp Neurol 240:153–160. CrossRef Medline

Chaplan SR, Bach FW, Pogrel JW, Chung JM, Yaksh TL (1994) Quantitative assessment of tactile allodynia in the rat paw. J Neurosci Methods 53:55–63. CrossRef Medline

Chen H, Lun Y, Ovchinnikov D, Kokubo H, Oberg KC, Pepicelli CV, Gan L, Lee B, Johnson RL (1998) Limb and kidney defects in Lmx1b mutant mice suggest an involvement of LMX1B in human nail patella syndrome. Nat Genet 19:51–55. CrossRef Medline

Chen ZF, Rebelo S, White F, Malmberg AB, Baba H, Lima D, Woolf CJ, Basbaum AI, Anderson DJ (2001) The paired homeodomain protein DRG11 is required for the projection of cutaneous sensory afferent fibers to the dorsal spinal cord. Neuron 31:59–73. CrossRef Medline

Cheng L, Arata A, Mizuguchi R, Qian Y, Karunaratne A, Gray PA, Arata S, Shirasawa S, Bouchard M, Luo P, Chen CL, Busslinger M, Goulding M, Onimaru H, Ma Q (2004) Tlx3 and Tlx1 are post-mitotic selector genes determining glutamatergic over GABAergic cell fates. Nat Neurosci 7:510–517. CrossRef Medline

Cheng L, Samad OA, Xu Y, Mizuguchi R, Luo P, Shirasawa S, Goulding M, Ma Q (2005) Lbx1 and Tlx3 are opposing switches in determining GABAergic versus glutamatergic transmitter phenotypes. Nat Neurosci 8:1510–1515. CrossRef Medline

Craig AD (2003) Pain mechanisms: labeled lines versus convergence in central processing. Annu Rev Neurosci 26:1–30. CrossRef Medline

Dado RJ, Katter JT, Giesler GJ Jr (1994) Spinothalamic and spinohypothalamic tract neurons in the cervical enlargement of rats: II. Responses to innocuous and noxious mechanical and thermal stimuli. J Neurophysiol 71:981–1002. Medline

Dai JX, Hu ZL, Shi M, Guo C, Ding YQ (2008) Postnatal ontogeny of the transcription factor Lmx1b in the mouse central nervous system. J Comp Neurol 509:341–355. CrossRef Medline

Davidson S, Truong H, Giesler GJ Jr (2010a) Quantitative analysis of spinothalamic tract neurons in adult and developing mouse. J Comp Neurol 518:3193–3204. CrossRef Medline

Davidson S, Truong H, Nakagawa Y, Giesler GJ Jr (2010b) A microinjection technique for targeting regions of embryonic and neonatal mouse brain in vivo. Brain Res 1307:43–52. CrossRef Medline

Deacon RM (2013) Measuring the strength of mice. J Vis Exp 2:76. CrossRef Medline

Ding YQ, Yin J, Kania A, Zhao ZQ, Johnson RL, Chen ZF (2004) Lmx1b controls the differentiation and migration of the superficial dorsal horn neurons of the spinal cord. Development 131:3693–3703. CrossRef Medline

Doyle CA, Hunt SP (1999) Substance P receptor (neurokinin-1)-expressing neurons in lamina I of the spinal cord encode for the intensity of noxious stimulation: a c-Fos study in rat. Neuroscience 89:17–28. CrossRef Medline

Dreyer SD, Zhou G, Baldini A, Winterpacht A, Zabel B, Cole W, Johnson RL, Lee B (1998) Mutations in LMX1B cause abnormal skeletal patterning and renal dysplasia in nail patella syndrome. Nat Genet 19:47–50. CrossRef Medline

Duan B, Cheng L, Bourane S, Britz O, Padilla C, Garcia-Campmany L, Krashes M, Knowlton W, Velasquez T, Ren X, Ross SE, Lowell BB, Wang Y, Goulding M, Ma Q (2014) Identification of spinal circuits transmitting and gating mechanical pain. Cell 159:1417–1432. CrossRef Medline

Dunston JA, Reimschisel T, Ding YQ, Sweeney E, Johnson RL, Chen ZF, McIntosh I (2005) A neurological phenotype in nail patella syndrome (NPS) patients illuminated by studies of murine Lmx1b expression. Eur J Hum Genet 13:330–335. CrossRef Medline

Erlander MG, Tobin AJ (1991) The structural and functional heterogeneity of glutamic acid decarboxylase: a review. Neurochem Res 16:215–226. CrossRef Medline

Ferreira A, Rapoport M (2002) The synapsins: beyond the regulation of neurotransmitter release. Cell Mol Life Sci 59:589–595. CrossRef Medline

Francis JT, Xu S, Chapin JK (2008) Proprioceptive and cutaneous representations in the rat ventral posterolateral thalamus. J Neurophysiol 99:2291–2304. CrossRef Medline

Gauriau C, Bernard JF (2004) A comparative reappraisal of projections from the superficial laminae of the dorsal horn in the rat: the forebrain. J Comp Neurol 468:24–56. CrossRef Medline

Giesler GJ Jr, Spiel HR, Willis WD (1981) Organization of spinothalamic tract axons within the rat spinal cord. J Comp Neurol 195:243–252. CrossRef Medline

Hargreaves K, Dubner R, Brown F, Flores C, Joris J (1988) A new and sensitive method for measuring thermal nociception in cutaneous hyperalgesia. Pain 32:77–88. CrossRef Medline

Helms AW, Johnson JE (2003) Specification of dorsal spinal cord interneurons. Curr Opin Neurobiol 13:42–49. CrossRef Medline

Holstege JC, de Graaff W, Hossaini M, Cardona Cano S, Jaarsma D, van den Akker E, Deschamps J (2008) Loss of Hoxb8 alters spinal dorsal laminae and sensory responses in mice. Proc Natl Acad Sci U S A 105:6338–6343. CrossRef Medline

Hylden JL, Anton F, Nahin RL (1989) Spinal lamina I projection neurons in the rat: collateral innervation of parabrachial area and thalamus. Neuroscience 28:27–37. CrossRef Medline

Kao TJ, Kania A (2011) Ephrin-mediated cis-attenuation of Eph receptor signaling is essential for spinal motor axon guidance. Neuron 71:76–91. CrossRef Medline

Kobayashi Y (1998) Distribution and morphology of spinothalamic tract neurons in the rat. Anat Embryol 197:51–67. Medline

Li JL, Ding YQ, Shigemoto R, Mizuno N (1996) Distribution of trigeminothalamic and spinothalamic-tract neurons showing substance P

receptor-like immunoreactivity in the rat. Brain Res 719:207–212. CrossRef Medline

Li JL, Ding YQ, Xiong KH, Li JS, Shigemoto R, Mizuno N (1998) Substance P receptor (NK1)-immunoreactive neurons projecting to the periaqueductal gray: distribution in the spinal trigeminal nucleus and the spinal cord of the rat. Neurosci Res 30:219–225. CrossRef Medline

Lima D (2009) Ascending pathways: anatomy and physiology. In: Science of pain (Basbaum AI, Bushnell MC, eds), pp 477–526. Amsterdam: Elsevier.

Littlewood NK, Todd AJ, Spike RC, Watt C, Shehab SA (1995) The types of neuron in spinal dorsal horn which possess neurokinin-1 receptors. Neuroscience 66:597–608. CrossRef Medline

Mantyh PW, DeMaster E, Malhotra A, Ghilardi JR, Rogers SD, Mantyh CR, Liu H, Basbaum AI, Vigna SR, Maggio JE (1995) Receptor endocytosis and dendrite reshaping in spinal neurons after somatosensory stimulation. Science 268:1629–1632. CrossRef Medline

Mantyh PW, Rogers SD, Honore P, Allen BJ, Ghilardi JR, Li J, Daughters RS, Lappi DA, Wiley RG, Simone DA (1997) Inhibition of hyperalgesia by ablation of lamina I spinal neurons expressing the substance P receptor. Science 278:275–279. CrossRef Medline

Mizuguchi R, Kriks S, Cordes R, Gossler A, Ma Q, Goulding M (2006) Ascl1 and Gsh1/2 control inhibitory and excitatory cell fate in spinal sensory interneurons. Nat Neurosci 9:770–778. CrossRef Medline

Mogil JS, Ritchie J, Sotocinal SG, Smith SB, Croteau S, Levitin DJ, Naumova AK (2006) Screening for pain phenotypes: analysis of three congenic mouse strains on a battery of nine nociceptive assays. Pain 126:24–34. CrossRef Medline

Morgan MM, Sohn JH, Liebeskind JC (1989) Stimulation of the periaqueductal gray matter inhibits nociception at the supraspinal as well as spinal level. Brain Res 502:61–66. CrossRef Medline

Muzumdar MD, Tasic B, Miyamichi K, Li L, Luo L (2007) A global double-fluorescent Cre reporter mouse. Genesis 45:593–605. CrossRef Medline

Narayanan CH, Fox MW, Hamburger V (1971) Prenatal development of spontaneous and evoked activity in the rat (Rattus norvegicus albinus). Behaviour 40:100–134. CrossRef Medline

Oury F, Murakami Y, Renaud JS, Pasqualetti M, Charnay P, Ren SY, Rijli FM (2006) Hoxa2- and rhombomere-dependent development of the mouse facial somatosensory map. Science 313:1408–1413. CrossRef Medline

Pasqualetti M, Ren SY, Poulet M, LeMeur M, Dierich A, Rijli FM (2002) A Hoxa2 knockin allele that expresses EGFP upon conditional Cre-mediated recombination. Genesis 32:109–111. CrossRef Medline

Pillai A, Mansouri A, Behringer R, Westphal H, Goulding M (2007) Lhx1 and Lhx5 maintain the inhibitory-neurotransmitter status of interneurons in the dorsal spinal cord. Development 134:357–366. CrossRef Medline

Rebelo S, Reguenga C, Lopes C, Lima D (2010) Prrxl1 is required for the generation of a subset of nociceptive glutamatergic superficial spinal dorsal horn neurons. Dev Dyn 239:1684–1694. CrossRef Medline

Ren K, Ruda MA (1994) A comparative study of the calcium-binding proteins calbindin-D28K, calretinin, calmodulin and parvalbumin in the rat spinal cord. Brain Res Brain Res Rev 19:163–179. CrossRef Medline

Rozen S, Skaletsky H (2000) Primer3 on the WWW for general users and for biologist programmers. Methods Mol Biol 132:365–386. Medline

Schaeren-Wiemers N, Gerfin-Moser A (1993) A single protocol to detect transcripts of various types and expression levels in neural tissue and cultured cells: in situ hybridization using digoxigenin-labelled cRNA probes. Histochemistry 100:431–440. CrossRef Medline

Spike RC, Puskár Z, Andrew D, Todd AJ (2003) A quantitative and morphological study of projection neurons in lamina I of the rat lumbar spinal cord. Eur J Neurosci 18:2433–2448. CrossRef Medline

Todd AJ (2010) Neuronal circuitry for pain processing in the dorsal horn. Nat Rev Neurosci 11:823–836. CrossRef Medline

Todd AJ, Spike RC (1993) The localization of classical transmitters and neuropeptides within neurons in laminae I-III of the mammalian spinal dorsal horn. Prog Neurobiol 41:609–645. CrossRef Medline

Todd AJ, Spike RC, Polgár E (1998) A quantitative study of neurons which express neurokinin-1 or somatostatin sst2a receptor in rat spinal dorsal horn. Neuroscience 85:459–473. CrossRef Medline

Todd AJ, McGill MM, Shehab SA (2000) Neurokinin 1 receptor expression by neurons in laminae I, III and IV of the rat spinal dorsal horn that project to the brainstem. Eur J Neurosci 12:689–700. CrossRef Medline

Todd AJ, Puskar Z, Spike RC, Hughes C, Watt C, Forrest L (2002) Projection neurons in lamina I of rat spinal cord with the neurokinin 1 receptor are selectively innervated by substance p-containing afferents and respond to noxious stimulation. J Neurosci 22:4103–4113. Medline

Villeda SA, Akopians AL, Babayan AH, Basbaum AI, Phelps PE (2006) Absence of Reelin results in altered nociception and aberrant neuronal positioning in the dorsal spinal cord. Neuroscience 139:1385–1396. CrossRef Medline

Wang X, Babayan AH, Basbaum AI, Phelps PE (2012) Loss of the Reelin-signaling pathway differentially disrupts heat, mechanical and chemical nociceptive processing. Neuroscience 226:441–450. CrossRef Medline

Wang X, Zhang J, Eberhart D, Urban R, Meda K, Solorzano C, Yamanaka H, Rice D, Basbaum AI (2013) Excitatory superficial dorsal horn interneurons are functionally heterogeneous and required for the full behavioral expression of pain and itch. Neuron 78:312–324. CrossRef Medline

Witschi R, Johansson T, Morscher G, Scheurer L, Deschamps J, Zeilhofer HU (2010) Hoxb8-Cre mice: a tool for brain-sparing conditional gene deletion. Genesis 48:596–602. CrossRef Medline

Xiang CX, Zhang KH, Johnson RL, Jacquin MF, Chen ZF (2012) The transcription factor, Lmx1b, promotes a neuronal glutamate phenotype and suppresses a GABA one in the embryonic trigeminal brainstem complex. Somatosens Mot Res 29:1–12. CrossRef Medline

Xiang C, Zhang KH, Yin J, Arends JJ, Erzurumlu RS, Jacquin MF, Chen ZF (2010) The transcription factor, Lmx1b, is necessary for the development of the principal trigeminal nucleus-based lemniscal pathway. Mol Cell Neurosci 44:394–403. CrossRef Medline

Xu Y, Lopes C, Wende H, Guo Z, Cheng L, Birchmeier C, Ma Q (2013) Ontogeny of excitatory spinal neurons processing distinct somatic sensory modalities. J Neurosci 33:14738–14748. CrossRef Medline

Yuge K, Kataoka A, Yoshida AC, Itoh D, Aggarwal M, Mori S, Blackshaw S, Shimogori T (2011) Region-specific gene expression in early postnatal mouse thalamus. J Comp Neurol 519:544–561. CrossRef Medline

Zhao ZQ, Scott M, Chiechio S, Wang JS, Renner KJ, Gereau RW 4th, Johnson RL, Deneris ES, Chen ZF (2006) Lmx1b is required for maintenance of central serotonergic neurons and mice lacking central serotonergic system exhibit normal locomotor activity. J Neurosci 26:12781–12788. CrossRef Medline

Zylka MJ, Rice FL, Anderson DJ (2005) Topographically distinct epidermal nociceptive circuits revealed by axonal tracers targeted to Mrgprd. Neuron 45:17–25. CrossRef Medline